Characterization of a Novel MMS-Sensitive Allele of *Schizosaccharomyces pombe* mcm4+

Nimna S. Ranatunga and Susan L. Forsburg[1]
Program in Molecular and Computational Biology, University of Southern California, Los Angeles, California 90089
ORCID ID: 0000-0002-4895-8598 (S.L.F.)

ABSTRACT The minichromosome maintenance (MCM) complex is the conserved helicase motor of the eukaryotic replication fork. Mutations in the Mcm4 subunit are associated with replication stress and double strand breaks in multiple systems. In this work, we characterize a new temperature-sensitive allele of *Schizosaccharomyces pombe* mcm4+. Uniquely among known *mcm4* alleles, this mutation causes sensitivity to the alkylation damaging agent methyl methanesulfonate (MMS). Even in the absence of treatment or temperature shift, *mcm4-c106* cells show increased repair foci of RPA and Rad52, and require the damage checkpoint for viability, indicating genome stress. The *mcm4-c106* mutant is synthetically lethal with mutations disrupting fork protection complex (FPC) proteins Swi1 and Swi3. Surprisingly, we found that the deletion of *rif1+* suppressed the MMS-sensitive phenotype without affecting temperature sensitivity. Together, these data suggest that *mcm4-c106* destabilizes replisome structure.

The MCM helicase comprises six related proteins (Mcm2–7) that form a highly conserved heterohexameric ring functioning as the primary unwinding activity in the eukaryotic replisome (reviewed in Abid Ali and Costa 2015; O'Donnell and Li 2016). The loading of the MCM complex specifies potential replication origins. Replication initiation occurs with assembly of active replicative helicase known as CMG (Cdc45-Mcm-GINS). The helicase travels with other replisome components (Gambus *et al.* 2009). Recent studies examining the structure of the active CMG complex have provided insight into its mechanism. Cdc45 and GINS are activating agents (Moyer *et al.* 2006; Ilves *et al.* 2010) that bind at the Mcm2-Mcm5 "gate" where the MCM ring opens and closes around DNA (Costa *et al.* 2011, 2014; Sun *et al.* 2015). CMG makes direct contacts at the leading C-terminal side of the MCM ring with DNA polymerase ε, which is the processive leading strand polymerase (Langston *et al.* 2014; Sun *et al.* 2015). The DNA polymerase α/primase complex that initiates lagging strand synthesis is coupled to CMG via a trimeric protein called Mcl1 (Sc Ctf4, Hs AND-1) (Simon *et al.* 2014). Another conserved protein, Mrc1 (Hs Clapsin), is thought to help maintain the coupling with DNA polymerase Epsilon (Lou *et al.* 2008). The Swi1-Swi3 complex (Hs Timeless-Tipin, Sc Tof1-Csm3), called the Fork Protection Complex (FPC), also acts with Mrc1 and travels with the replisome (reviewed in Leman and Noguchi 2012). The FPC is not essential for viability in the yeasts, but in its absence, cells show uncoupling of the replisome and increased ssDNA formation, disruption in activation of the replication checkpoint, sensitivity to DNA damaging agents, and defects in cohesin (reviewed in Leman and Noguchi 2012).

The Mcm4 subunit resides on the opposite side of the MCM ring from the Mcm2–5 gate that binds Cdc45 and GINS, near the proposed lagging strand template (reviewed in O'Donnell and Li 2016). Interestingly, numerous mutations in this subunit have been linked to genome instability in mammalian systems. The point mutation F345I (*chaos3*), located downstream of the Zn-finger motif of MCM4 in mouse, is associated with mammary carcinoma (Shima *et al.* 2007). The *mcm4-D573H* mutation is associated with T cell lymphoblastic leukemia/lymphoma in a mouse model (Bagley *et al.* 2012), and *mcm4-G364R* in humans is associated with skin cancer (Ishimi and Irie 2015). All these mutations are related with increased double strand breaks, and in some cases formation of micronuclei. N-terminally truncated Mcm4 (Δ1–50) is linked to glucocorticoid deficiency and defective DNA repair in humans (Hughes *et al.* 2012; Gineau *et al.* 2012). Although the primary sequence of the Mcm4 N-terminus is neither conserved nor essential, this domain appears to be a common substrate for the DDK kinase required to initiate replication (Masai *et al.* 2006; Sheu and Stillman 2006). In budding yeast, deletion of the N-terminus bypasses a requirement for DDK, suggesting

that DDK overcomes an inhibitory function (Sheu and Stillman 2010). The N-terminus is also important for regulating fork progression when cells have depleted nucleotide pools during hydroxyurea (HU) treatment (Devault *et al.* 2008; Sheu *et al.* 2014). C-terminal truncations of Mcm4 also cause HU sensitivity, and fail to restrain single-stranded DNA accumulation (Nitani *et al.* 2008).

The fission yeast *mcm4$^+$* (*cdc21$^+$*) gene was originally identified in a screen for temperature-sensitive *cdc* mutants that arrest as elongated cells with undivided nuclei at the restrictive temperature (Nasmyth and Nurse 1981; Coxon *et al.* 1992). These *mcm4-M68* cells accumulate approximately 2C DNA content, and show evidence of DNA damage including DNA double strand breaks and generating a robust checkpoint-dependent arrest (Nasmyth and Nurse 1981; Coxon *et al.* 1992; Liang *et al.* 1999; Bailis *et al.* 2008; Sabatinos *et al.* 2015). Viability is low upon return to permissive temperature, suggesting that this damage is irreversible (Liang *et al.* 1999; Bailis *et al.* 2008). The 2C DNA content observed in *mcm4-M68* suggests that cells are competent for replication initiation and the bulk of DNA replication at the restrictive temperature. A second temperature-sensitive allele was constructed by fusing a *degron* cassette to *mcm4-M68* (Lindner *et al.* 2002). This enhances protein turnover leading to a rapid inactivation at restrictive temperature, and cells arrest with a 1C DNA content (Lindner *et al.* 2002; Bailis *et al.* 2008; Sabatinos *et al.* 2015). However, despite evidence of DNA damage including large RPA and Rad52-containing "megafoci," *mcm4-dg* cells continue to divide, indicating that they have evaded the damage checkpoint (Sabatinos *et al.* 2015). Survivors show dramatic evidence for chromosome mis-segregation, abnormal nuclear division, and chromosome rearrangement (Sabatinos *et al.* 2015).

A large C-terminal truncation mutant, *mcm4-c106*, is both temperature-sensitive and HU-sensitive (Nitani *et al.* 2008). In this study, we show that, unlike other mutant alleles of *mcm4*, *mcm4-c106* is also sensitive to the alkylating agent MMS. Moreover, the phenotype of *mcm4-c106* at the restrictive temperature with high viability is distinct from that of the other temperature-sensitive alleles. Genetic interactions and synthetic lethality with components of the fork protection complex suggest that the *mcm4-c106* truncation mutation leads to specific defects in maintaining replisome structure, causing genome instability.

MATERIALS AND METHODS

Cell growth and cultures

Fission yeast strains are listed in Table 1. All strains were maintained according to standard protocols (Sabatinos and Forsburg 2010). Strains were grown in YES or Edinburgh minimal medium (EMM) with ammonium chloride as the nitrogen source, supplemented with the required nutrients at 25° unless otherwise stated. For all experiments, cultures were grown in 5 ml of liquid media from a single colony at 25° overnight and released to fresh media and grown at 25° to midlog phase. Serial dilutions and plating assays were performed in cultures grown in YES, while the imaging experiments were performed in cultures grown in EMM.

Serial dilution assays and relative viability

For serial dilutions, cell cultures were grown in 5 ml of YES from a single colony at 25° overnight, to midexponential phase. Cells were counted and fivefold serial dilutions were spotted onto plates to assess drug or temperature sensitivity. Drug plates were allowed to grow for 3–5 d at 25° before scanning on a flatbed scanner. The experiments were repeated at least twice. For relative viability, cells at $OD_{595} \sim 0.3$ were

treated with 0.01% MMS for 4–6 hr or shifted to 36° for 4–6 hr (as indicated in the figure legend). Samples were collected every 2 hr and fixed in 70% ethanol for Flow Cytometry (FACS) and DNA staining with DAPI. Serial dilutions of equal volumes were plated at selected time points and allowed to grow at 25° for 5 d before counting viable colonies.

Protein extractions

Western blot analysis was performed using cultures grown to early log phase ($OD_{595} \sim 0.3$) in YES at 25°. Cultures were split into equal volumes and treated with 0.01% MMS or left untreated for 4 hr at 25°. $10 \times$ stop buffer containing 2% sodium azide was added and cultures were incubated on ice for 10 min before harvesting the cells. Cells were subsequently washed twice with $1 \times$ PBS and whole cell proteins were extracted using trichloric acid (TCA) (Foiani *et al.* 1994). The extractions were quantified using a Pierce BCA Kit. 80–100 μg of protein was loaded on 8% SDS-PAGE gels. Primary antibody for Chk1HA (16B12 anti-HA; Covance or anti-HA; Abcam) were used in 1:1500 dilutions overnight at 4°. Mcm4 protein levels were detected with antibody purified from rabbit serum 5898 diluted 1:3000 (Sherman *et al.* 1998) incubated at 4° overnight. After washing with PBST, anti-mouse-IgG-HRP secondary antibody sigma) was used to detect HA in a 1:5000 dilution, while a 1:5000 dilution of anti-rabbit-HRP (BD Biosciences) incubated for 1 hr at room temperature was used in Mcm4 detection. 1:1500 PCNA anti-mouse (Santa Cruz) was used as the loading control.

Pulse field gel electrophoresis (PFGE)

PFGE was performed to separate full-length chromosomes using a BioRad Chef II Pulse Field Machine. 50 ml cultures grown to early log phase ($OD_{595} \sim 0.3$–0.4) were shifted to 36° for 4 hr and released to permissive temperature 25° for 2 hr. For the MMS treatment, the cells were treated with 0.01% MMS for 4 hr and released to media lacking MMS for 2 hr for recovery after washing out the drug from the cultures. Cells were treated with $10 \times$ stop buffer containing 2% sodium azide and placed on ice for 5 min before harvesting the cells. Harvested cells were washed with $1 \times$ PBS and CSE buffer (20 mM Citric Acid, 20 mM Na_2HPO_4, 40 mM EDTA, and 1.2 M sorbitol; at pH 5.6, sterilized, and stored at room temperature). Each culture was digested with 0.2 mg/ml 20T Zymolase and 0.45 mg/ml lysing enzyme (Sigma) in CSE. Digested cells were used to prepare plugs that were resuspended in $1 \times$ TSE (10 mM Tris pH 7.5, 45 mM EDTA pH 8.0, and 0.9 M Sorbitol). Plugs were treated with 5 ml of 1 mg/ml proteinase K Sarkosyl/EDTA at 55° for 48 hr (1% Sarkosyl and 0.5 M EDTA pH 9.5). The buffer was changed after 24 hr of incubation and washed four times (30 min each) with $1 \times$ TE. Plugs were washed with $1 \times$ TAE prior to running the gels. Gels were run for 48 hr using 2 V/cm, 1200–1800-sec switch time, and a 106° angle. DNA was visualized via ethidium bromide staining.

FACS

FACS was performed as described in (Sabatinos and Forsburg 2015). Briefly, cells were fixed in 70% ice cold ethanol, washed with 50 mM sodium citrate, and resuspended in 50 mM sodium citrate with 0.1 mg/ml RNAse. Samples were next stained with 1 μM Sytox Green (Invitrogen) in 50 mM sodium citrate, and sonicated at 20% amplitude for 5 sec. Samples were analyzed by running on a Becton Dickinson FACScan flow cytometer.

Microscopy

Cultures were grown in EMM supplement with ammonium chloride. Agar pads were prepared as described in Green *et al.* (2015). Images of live cells were acquired with a DeltaVision Core (Applied Precision, Issaquah, WA) microscope using a $60 \times$ N.A. 1.4 PlanApo objective lens and a 12-bit Photometrics CoolSnap HQII CCD. The system

Strain	Genotype	Source
FY 7	h- 972	Our stock
FY 527	h-his3-D1 ade6-M216 ura4-D18 leu1-32	Our stock
FY 528	h+ his3-D1 ade6-M210 ura4-D18 leu1-32	Our stock
FY 261	h+ can1-1 leu1-32 ade6-M216 ura4-D18	Our stock
FY 784	h+ cdc21-M68 ura4-D18 leu1-32 ade6-M210 can1-1 (mcm4)	Our stock
FY 4241	h- cdc21-c106:kan	Takuro Nakagawa
FY 4311	h- cdc21-c106::kan ura4-D18 his3-D1 ade6- M210	Our stock
FY 4310	h- cdc21-c84::kan Ura4-D18 his3-D1	Our stock
FY 5942	h- cdc21-c106::HphMx ura4-D18 his3-D1 ade6- M210	This work
FY 3395	h- mcm4(cdc21-M68)-ts-dg::ura4+ ura4-D18	Our stock
FY 6126	h+ cdc21-c106::kan ura4-D18 his 3D-1 leu1-32 ade6-M210	Our stock
FY 6038	h- pcn1-K164R::ura4 cdc21-c106::kan ura4-D18 ade6-M210	Our stock
FY 6039	h+kpa1Δ::bleMX6 cdc21-c106::kan his4- 239/his3-D1 ade6-M26 ?(kpa1)	Our stock
FY 6040	h+Δrhp18::ura4 cdc21-c106::kan ura4-D18 leu1- 32 ade6-704	This work
FY 6041	h- Δreb1::kanMX cdc21-c106::HphMx his 3-D1 ura4-D18 ade6-M210	This work
FY 6042	h+Δreb1::kanMX cdc21-c106::HphMx ura4-D18 leu1-32 ade6-M216	This work
FY 6043	h- cdc21-c106::kan cyc17::ura4 his3 D-1 ade6- M216 ura4 cyc17 = allelic to cig2	This work
FY 6044	h+ cdc21-c106::kan cyc17::ura4 his3 D-1 ade6- M216 leui1-32 ura4	This work
FY 6052	h+ Δrev1::ura4+ cdc21-c106::kan ura4-D18 his3-D1 ade6-M216/210?ura4-D18	This work
FY 6053	h- Δrev1::ura4+ cdc21-c106::kan ura4-D18 his3? ade6-M?ura4-D18	This work
FY 6054	h- eso1-etaΔ::kanMX6 cdc21-c106::HphMx ura4- D18 his3-D1 ade6-M210	This work
FY 6055	h- eso1-etaΔ::kanMX6 cdc21-c106::HphMx ura4- D18 his3-D1 ade6-M210 Leu1-32	This work
FY 6077	h+ Δrad8::hphMX cdc21-c106::kan ura4-D18 his3-D1 ade6-M216 leu1-32	This work
FY 6078	h- Δbrc1::ura4+ cdc21-c106::kan ura4-D18 ade6-M210	This work
FY 6079	h-Δbrc1::ura4+ cdc21-c106::kan ura4-D18 his 3- D1 ade6-M210	This work
FY 6080	h+ ΔUbc13::ura4+ cdc21-c106::kan his3D18 ura4-D18 ade6-m210	This work
FY 6123	h- cdc21-c106::kan rev3::hphMX6 ura4-D18 his3-D1 ade6-M210	This work
FY 6146	h+srs2::kan cdc21-c106::HphMx ade6-M210 leu1-32 ura4-D18 his3-D1	This work
FY 6147	h-srs2::kan cdc21-c106::HphMx ade6-M210 ura4- D18 his3-D1	This work
FY6238	h+ cdc21-c106::HphMx ura4-D18 his3-D1 leu1- 32 ade6-M210	This work
FY 6248	h+Δ mms2::leu2 cdc21-c106::kan ura4-D18 leu1- 32 his4-239 ade6-M26	This work
FY 6266	h-cdc21-c106::kan rad11-Cerulean::hphMX rad22-YFP-natMX ura4-D18 leu1-32 ade6-M210	This work
FY 6281	h-cdc21-c106::kan chk1HA(ep) ade6-M216 ura4- D18 leu1-32 his 3D-1	This work
FY 6308	h+ cdc21-c106::kan Δcds1::ura4+ ura4-D18 leu1- 32 his3-D1 ade6-M210	This work
FY 6309	h- cdc21-c106::kan Δcds1::ura4+ ura4-D18 his3- D1 ade6-M210	This work
FY 6751	h+ cdc21-c106::kan mad2D::ura4+ ade6-M210 leu1-32 ura4-D18	This work
FY 6777	h- cdc21-c106::HphMx Δrif1:kanMX6-Bioneer ura4-D18 ade6-M210 his3-D1	This work
FY 6778	h+ cdc21-c106::HphMx Δrif1:kanMX6-Bioneer ura4-D18 ade6-M210 his3-D1	This work
FY 6779	h- cdc21-c106::kan exo1::ura4 ura4-D18 ura4- D18 ade6-M210	This work
FY 6780	h+ cdc21-c106::kan exo1::ura4 ura4-D18 ura4- D18 ade6-M210	This work
FY 6961	h- swi6::ura4+ cdc21-c106::Kan leu1-32 ura4- (DS/E or D18?) ade6-M210 *can1-1*	This work
FY 7045	h+ cdc21-c106::kan fml1::natMX4 ura4-D18 his 3D-1 leu1-32 ade6-M210/216?	This work
FY 7047	cdc21-c106::kan fml1::natMX4 ura4-D18 his 3D- 1 leu1-32 ade6-M210/216	This work
FY 7048	h- chp1::kanMX6-Bioneer cdc21-c106::HphMx his3-D1 leu1-32 ura4-D18 ade6-M216/210?	This work
FY 7165	h- Δmus81::KanMX cdc21-c106::HphMx ura4- D18 his3-D1 ade6-M210	This work
FY 7166	h+ Δmus81::KanMX cdc21-c106::HphMx ura4- D18 his3-D1 ade6-M210	This work
FY 7461	h- mcl1-11 cdc21-c106::kan ade6-704 ura4-294 leu1-32 his3D-1	This work
FY 7462	h+mcl1-11 cdc21-c106::kan ade6-704 ura4-294 leu1-32 his3D-1	This work
FY7611	h+ rhp51::ura4+ cdc21-c106::kan ade6-704/ade 6-M210 leu1-32 ura4-D18	This work
FY 7802	h+ Δchl1::kanMX6-Bioneer cdc21-c106::HphMx his3-D1 leu1-32 ura4-D18 ade6-M210	This work
FY 7922	h+ arg3+::ccr1N-mCherry((D817 aa1-275))::his5+ cdc21-c106::kan rad11-Cerulean::hphMX rad22- YFP-natMX ura4-D18 his5D leu1-32 ade6- M210	This work
FY 7923	h- Δrif1::ura4+ Δswi1::KanMX ura4-D18 leu1-32 ade6-M210 his3-D1	This work
FY 7924	h+ Δrif1::ura4+ Δswi1::KanMX ura4-D18 leu1-32 ade6-M210 his3-D1	This work
FY 7925	h-Δrif1::ura4+ Δswi3::KanMX ura4-D18 leu1-32 ade6-M210 his3-D1	This work
FY 7926	h+Δrif1::ura4+ Δswi3::KanMX ura4-D18 leu1-32 ade6-M210 his3-D1	This work
FY 3664	h+ mcm4-"chaos" ura4-D18 leu1-32 ade6-M210	Our Stock
FY 8000	h+/− hht1-mRFP:kanMX his7+::lacI-GFP lys1+::lacO cdc21-c106-HphMx leu1-32 ura4- D18	This work

(continued)

Strain	Genotype	Source
FY 8015	*h+ Δctf8::kanMX6-Bioneer cdc21-c106::HphMx his 3-D1 ura4-D18 Leu1-32 ade6-M210*	This work
FY 8016	*h- Δctf8::kanMX6-Bioneer cdc21-c106::HphMx his 3-D1 ura4-D18 Leu1-32 ade6-M210*	This work
FY 8017	*h+ Δctf18::kanMX6-Bioneer cdc21-c106::HphMx ura4-D18 Leu1-32 ade6-M210*	This work
FY 8018	*h-Δctf18::kanMX6-Bioneer cdc21-c106::HphMx ura4-D18 Leu1-32 ade6-M210?*	This work
FY 7689	*h+ Δctf18::kanMX6-Bioneer ura4-D18 Leu1-32 ade6-M210?*	Our stock/Bioneer derived
FY 7690	*h- Δctf18::kanMX6-Bioneer ura4-D18 Leu1-32 ade6-M210?*	Our stock/Bioneer derived
FY 8107	*h+/−? cdc20-M10 cdc21-c106::kan ura4-D18 ade6- M210 leu1-32 his3-D1 (polε)*	This work
FY 7808	*h+ rad21-K1::ura4+ cdc21-c106::kan ura4-D18 leu1-32 ade6-M216 his7-366/his 3D-1*	This work
FY 8108	*h+/− ? Δrad22::ura4+ cdc21c-106::kan ura4-D18 leu1-32 his3-D1 arg3-D4*	This work
FY 5014	*h+ pcn1-K164R::ura4 ura4-D18 leu1-32 ade6- M210*	Our stock
FY 5270	*h+ kpa1Δ::bleMX6 his4-239 ade6-M26*	Our stock
FY 3124	*h+ Δrhp18::ura4+ ura4-D18 leu1-32 ade6-704*	Our stock
FY 4415	*h+ Δreb1::kanMX ade6-M216 ura4-D18 leu1-32*	Our stock
FY 277	*h+ cyc17::ura4 ade6-M216 leu1 ura4 cyc17 is allelic to cig2*	Hiroto Okayama
FY 5401	*h+ Δrev1::ura4+ ura4-D18 his4-239 ade6-M26*	Our stock
FY 4937	*h+ eso1::kanMX6 ura4-D18 leu1-32 ade-M210*	Our stock
FY 5142	*h+ Δbrc1::ura4+ ura4-D18 leu1-32 ade6- M210*	Mathew O'Connell
FY 4938	*h+ rev3::hphMX6 ura4-D18 leu1-32 ade6- M210*	Our stock
FY 2050	*h+ srs2::kan ade6-M210 leu1-32 ura4-D18*	Our stock
FY 5260	*h- Δ mms2::leu2 leu1-32 his4-239 ade6-M26*	Our stock
FY 5625	*h+ Δrad8::hphMX leu1-32 ura4-D18 ade6- M216 his3-D1*	Our stock/Bioneer derived
FY 4742	*h- rad11-Cerulean::hphMX rad22-YFP-natMX leu1-32 ade6-M210 ura4-D18 (rad11 = ssb1)*	Our stock
FY 4611	*h- chk1HA(ep) ade6-M216 ura4-D18 leu1-32*	Our stock
FY 1163	*h- rad12::ura4+ ade6-M210 leu1-32 ura4-D18*	Our stock
FY 3845	*h-leu1-32::hENT1-leu1+(pJAH29) his7-366::hsv-tk- his7+(pJAH31) ura4-D18 ade6-M216*	Our stock
FY 1257	*h+ mad2D::ura4+ ade6-M210 leu1-32 ura4-D18*	Shelly Sazer
FY 5583	*h+ Δrif1::kanMX6-Bioneer leu1-32 ura4-D18 ade6- M210 his3-D1*	Our stock/Bioneer derived
FY 3884	*h- exo1::ura4 ura4-D18*	Mathew O'Connell
FY 2389	*h- leu1-32 ura4-D18 Δrif1::ura4+*	Junko Kanoh
FY5555	*h- Δfml1::natMX4 ura4-D18 his3-D1 leu1-32*	Our stock
FY 4581	*h- chp1::kanMX6-Bioneer leu1-32 ura4-D18 ade6-M216his3-D1*	Our stock
FY4159	*h+ Δmus81::KanMX*	Our stock
FY1191	*h- mcl1-11 ade6-704 ura4-294 leu1-32 (ts)*	Dwight Williams
FY 1203	*h+ rhp51::ura4+ ade6-704 leu1-32 ura4-D18*	Greg Freyer
FY 1318	*h+ rec8::ura4+ ura4-D18 leu1-32 ade6-M210*	Our Stock
FY 1159	*h-rad21-K1::ura4+ ura4-D18 leu1-32 ade6-M216 his7-366*	Our stock
FY 3588	*h- arg3+::ccr1N-mCherry((D817 aa1-275)::his5+ ura4-D18 his5D*	Zach Cande/XieTang
FY 3227	*h+ Δswi1::KanMX ura4-D18 leu1-32 ade6-M210 his3-D1*	Our stock
FY 3228	*h+ Δswi3::KanMX ura4-D18 leu1-32 ade6-M210 his3-D1*	Our Stock
FY 7995	*h? arg3+::ccr1N-mCherry((D817 aa1-275))::his5+ rad11-Cerulean::hphMX rad22-YFP-kanMX ura4-D18 his5D leu1-32*	This work
FY 5787	*h+ hht1-mRFP:kanMX his7+::lacI-GFP lys1+::lacO leu1-32 ura4-D18*	Our stock
FY 7653	*h+ Δctf8::kanMX6-Bioneer his 3-D1 ura4-D18 Leu1-32 ade6-M210?*	Our stock/Bioneer derived
FY 8017	*h+ Δctf18::kanMX6-Bioneer cdc21-c106::HphMx ura4-D18 Leu1-32 ade6-M210*	This work/Bioneer derived
FY 8110	*h?psf2-209 cdc21-c106::Kan ura4-D18leu1-32 ade6-M216*	This work
FY 8111	*h? rad35-271 cdc21-c106::Kan ura4-D18 leu1-32 ade6-M216*	This work
FY 2711	*h+ psf2-209 ura4-D18 ade6-M216 leu1-32*	Our stock
FY 3999	*h+ rad35-271 allelic to dfp1*	Our stock
FY 8197	*h- pol1-1 cdc21-c106::Kan ura4-D18 leu1-32 ade6-M210 his3-D1*	This work
FY 1110	*h+ pol1-1 ura4-D18 leu1-32 ade6-M210*	Our stock

x-y pixel size is 0.109 μm. SoftWoRx v4.1 (Applied Precision, Issaquah, WA) software was used at acquisition. The image acquisition consisted of 13 Z-stacks with 0.5 μm for visualizing Rad11 and Rad52 foci at 36° and MMS. Cells were visualized at the asynchronous stage; 4 hr post-treatment and 2 hr postrelease from the treatment. Movies were captured to look at the replication dynamics in real time. Eighteen Z-stacks with 0.5 μm were acquired 10 min apart for the length of the experiment. The temperature was controlled at 25° if not specified. For still imaging, CFP was excited and detected with an (ex)438/24, (em)470/24 filter set and a 0.5 sec exposure excitation intensity attenuated to 10%; and YFP was excited and detected with an (ex)513/17, (em)559/38 filter set and a 0.5 sec exposure excitation intensity attenuated to 32%. Suitable polychroic mirrors were used. Ten 0.5 μm serial z-sections were captured. 3-D stacks were deconvolved with manufacturer-provided OTFs using a

constrained iterative algorithm, images were maximum intensity projected for presentation. Images were contrast adjusted using a histogram stretch with an equivalent scale and γ for comparability.

Data availability

Strains are available upon request. The authors state that all data necessary for confirming the conclusions presented in the article are represented fully within the article.

RESULTS

Identification of an MMS-sensitive allele of mcm4+

Mutants with defects in replisome components often show sensitivity to DNA damaging agents, but not all mutants are sensitive to all drugs. For example, in a recent study, we showed that cells deleted for nonessential helicases have distinct patterns of genotoxin sensitivity that establish a fingerprint for their roles in DNA replication and repair (Ding and Forsburg 2014). Here, we analyzed a panel of strains with different mutations in the essential mcm4+ gene for their sensitivity to different damaging agents, including: HU, which depletes nucleotide pools and causes fork stalling (Thelander and Reichard 1979); MMS, which is an alkylating agent that generates diverse lesions that block DNA polymerase (Lundin et al. 2005); and camptothecin (CPT), a topoisomerase inhibitor that leads to S-phase specific double strand breaks (Liu et al. 2000).

We examined the known temperature-sensitive alleles mcm4-M68, mcm4 dg, and mcm4-c106 (Nasmyth and Nurse 1981; Lindner et al. 2002; Nitani et al. 2008). The remaining mutants that we tested included a deletion of the N-terminal residues 2–73, a single point mutation (F346I) corresponding to the chaos allele in mouse (J. P. Yuan and S. L. Forsburg, unpublished data; Shima et al. 2007), and mcm4-4SA, which contains mutations in putative damage-specific phosphorylation sites S30A, S38A, S81A, and T95A (Figure 1A). As observed previously, some mcm4 mutants show sensitivity to HU, including the temperature-sensitive degron allele mcm4-dg, (Supplemental Material, Figure S1A) and the C-terminal truncation alleles mcm4-c84 and mcm4-c106 (Nitani et al. 2008). We did not observe CPT sensitivity in any of the strains (Figure S1B). Unexpectedly, however, we observed that the temperature-sensitive mcm4-c106 truncation is also sensitive to MMS exposure at the permissive growth temperature, which is not seen for any other mcm4 alleles (Figure 1B). Importantly, temperature-sensitive and MMS-sensitive phenotypes were not observed for the mcm4-c84 truncation, which contains a shorter truncation (Nitani et al. 2008). These results indicate that a larger C-terminus of Mcm4 is necessary for a proper response to MMS.

In general, sensitivity to MMS is observed in strains defective in checkpoint response or repair, and mutations that disrupt a distinct subset of replisome components. These include mutations affecting the fork protection complex (FPC) proteins Swi1 and Swi3, and the MCM kinase Hsk1/DDK that interacts with FPC (Memisoglu and Samson 2000; Noguchi et al. 2003, 2004; Kumar and Huberman 2004; Sommariva et al. 2005; Dolan et al. 2010). Given that mcm4-c106 shows sensitivity to MMS as well as to higher temperatures, we investigated both these phenotypes.

mcm4-c106 cells have a unique replication phenotype

There is no obvious difference in growth rate between wild-type and mcm4-c106 cells at permissive temperature (Figure 1A). To assess whether there is a subtle replication defect, we performed a classic minichromosome maintenance assay (Tye 1999). We transformed the wild-type, mcm4-M68, and mcm4-c106 strains with a
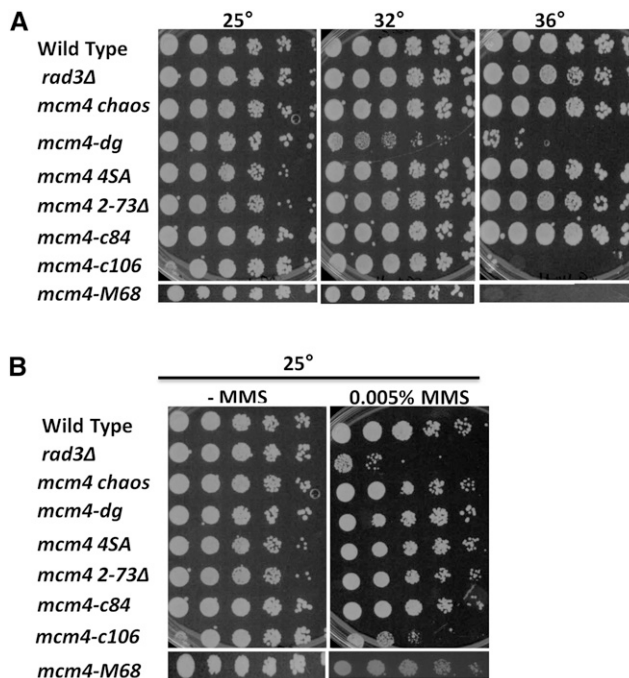

Figure 1 Viability of mcm4 mutants at 36° and in MMS. (A) Temperature sensitivity evaluated by 1:5 serially diluted cultures plated on YES (rich media) and grown at the indicated temperatures. Wild-type (FY 528), rad3Δ (FY1106), mcm4 chaos (FY 3664), mcm4-dg (FY 3395), mcm4-4SA (FY5251), mcm4 2-73Δ (FY 5688), mcm4-c84 (FY4310), mcm4-c106 (FY 4311), and mcm4-M68 (FY784). (B) MMS sensitivity evaluated by 1:5 serially diluted cultures plated on YES (rich media) as control and 0.005% MMS at 25°. MMS, methyl methanesulfonate; YES, yeast extract + supplements.

plasmid (pUR19N; Barbet et al. 1992) containing a single copy of Schizosaccharomyces pombe ars1 and compared the number of transformants/μg DNA (transformation efficiency) and plasmid stability (colony size). We found that both the number of transformed cells and the size of the colonies were reduced in mcm4-c106 compared to either mcm4-M68 or the wild type at permissive temperature (Figure 2). Additionally, we examined a plasmid with an additional ars (pDblet), which is intrinsically more stable (Brun et al. 1995). These transformants were larger than when transformed with a single ars plasmid (data not shown). These data suggest that mcm4-c106 suffers a defect in replication, even at permissive temperature.

At 36°, the canonical mcm4-M68 allele loses viability rapidly, with signs of DNA damage (Liang and Forsburg 2001; Bailis et al. 2008; Sabatinos et al. 2015). We examined the relative viability of mcm4-c106 following a shift to the restrictive temperature, and found that the loss of viability was more modest compared to mcm4-M68 (Figure 3A). We examined DNA accumulation using flow cytometry on cells that were arrested in G1 by nitrogen starvation, and released to the permissive temperature (25°) and the restrictive temperature (36°) (Figure 3B). We observed DNA accumulation to approximately 2C DNA content in both wild-type and mcm4-c106 cells, even at restrictive (36°) and nonrestrictive (25°) temperatures. This is similar to observations for the original mcm4-M68 temperature allele, which has a late S phase arrest (Nasmyth and Nurse 1981; Coxon et al. 1992; Bailis et al. 2008; Sabatinos et al. 2015).

However, the chromosome profiles observed in PFGE were strikingly different between these two mcm4 alleles. Typically, the chromosomes from cells with replication defects do not migrate normally at restrictive
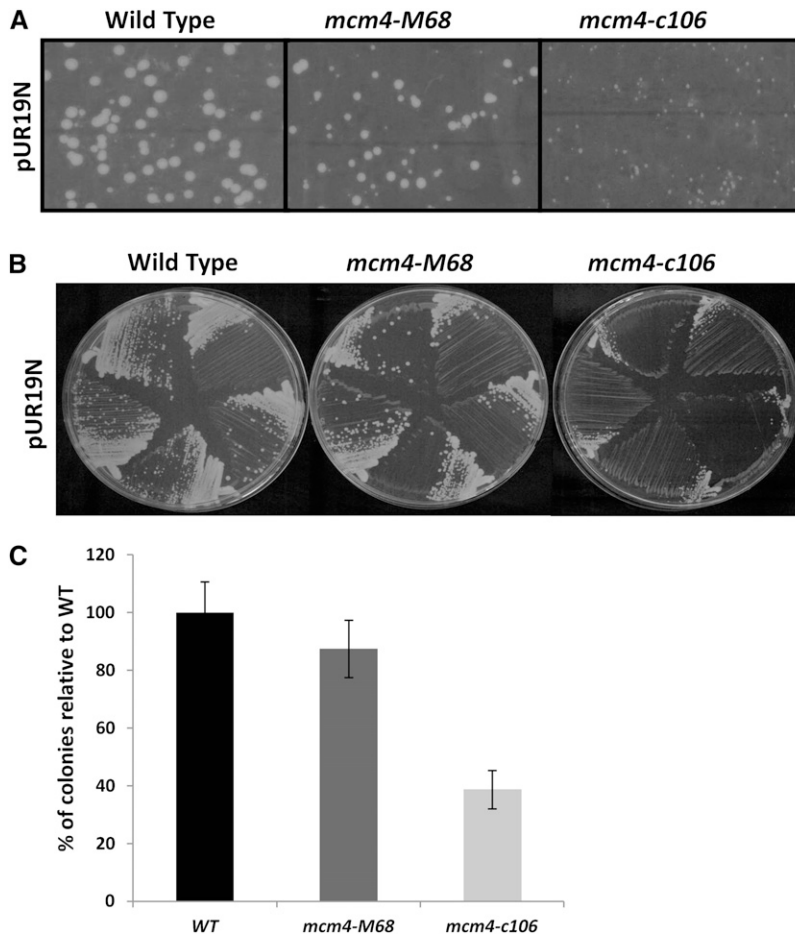
Figure 2 *mcm4-c106* has a defect in replication at permissive temperature. (A) WT (FY 528), *mcm4-M68* (FY784), and *mcm4-c106* (FY 4311) strains transformed with pUR19N plasmid plated on media lacking uracil. Colonies observed after 7 d of growth at 25°. (B) Colonies isolated from transformation (A), streaked to single colonies on media lacking uracil, and grown at 25° for 5 d. (C) Percentage of colonies observed posttransformation of 200 ng/µl pUR19N plasmid relative to the wild type. Error bars represent 95% C.I. of the mean. WT, wild-type.

temperature, either due to unresolved replication or recombination intermediates that preclude migration, or due to chromosome breakage (*e.g.*, Liang and Forsburg 2001; Waseem *et al.* 1992). Thus, as seen previously, the *mcm4-M68* chromosomes do not migrate at their normal position during a 36° temperature shift or upon release to 25°, but are replaced by a smear (Figure 3C, middle lanes). This is consistent with unresolved replication intermediates retarding gel migration, and the accumulation of double strand breaks as reported previously (Liang and Forsburg 2001; Bailis *et al.* 2008; Sabatinos *et al.* 2015). In contrast, *mcm4-c106* showed intact chromosomes under all conditions (Figure 3C, right lanes). This, along with the maintenance of viability and the ability to recover from temperature arrest, suggests that the nature of the temperature-sensitive defect in *mcm4-c106* is different from that of the well-studied *mcm4-M68*.

We observed loss of viability of *mcm4-c106* cells treated with MMS (Figure 3D) consistent with the MMS sensitivity observed in plate assays (Figure 1B). The loss of viability was relatively modest compared to a repair-defective allele of PCNA, *pcn1-K164R* (Frampton 2006). During MMS treatment in liquid culture at the permissive temperature, both wild-type and *mcm4-c106* mutants showed an S phase delay, as indicated by the intermediate peak that is observed in the FACS profiles (Figure 3B). In both wild-type and *mcm4-c106* cells treated with MMS and following release, we observed little if any migration of intact chromosomes into a PFGE gel (Figure S2).

Finally, we examined Mcm4 protein levels in the mutant. Loss of Mcm4 protein has been correlated with genomic instability (Liang and Forsburg 2001; Bailis *et al.* 2008; Sabatinos *et al.* 2015). However,

we saw no change in Mcm4 protein levels during MMS treatment or at 36° in *mcm4-c106* (Figure 4, C and D), suggesting that its temperature sensitivity and MMS phenotypes are not related to protein stability.

Chromosome segregation is normal in mcm4-c106

Recently, we showed that *mcm4 dg* mutants undergo division despite their replication defects, and this is accompanied by aberrant nuclear division, abnormal chromosome segregation, and reduced viability (Sabatinos *et al.* 2015). In contrast, we saw no evidence for abnormal mitosis in *mcm4-c106* cells. We determined segregation of chromosome I, using a *lacI*-GFP fusion in a strain with a *lacO* array at centromere I to generate a centromere proximal signal (Nabeshima *et al.* 1998). We observed no evidence for lagging chromosomes, or chromosome mis-segregation, indicating no substantial mitotic defects in *mcm4-c106* (Figure S3).

mcm4-c106 requires an intact damage checkpoint

The *mcm4-c106* cells elongate following treatment at 36° or in MMS, which suggests successful activation of the damage checkpoint. We verified this by monitoring the checkpoint kinase Chk1, which undergoes an activating phosphorylation that results in a mobility shift in SDS-PAGE (Walworth and Bernards 1996). We observed a shift in Chk1 in both wild-type and *mcm4-c106* cells treated with MMS (Figure 4A), and in wild-type and *mcm4-c106* cells at the restrictive temperature (Figure 4B), consistent with successful activation of Chk1 under both conditions in the mutant.
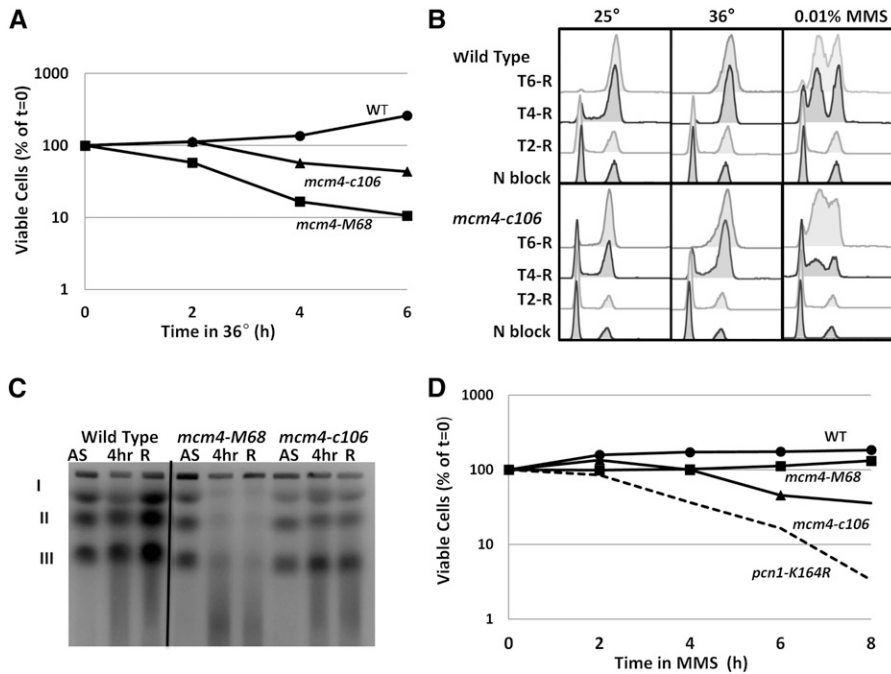
Figure 3 Replication dynamics in *mcm4-c106* at 36° and MMS. (A) Relative viability of cultures during incubation at 36°. The indicated cultures were plated at 25° on YES, and viability was compared to the starting culture. (B) Bulk DNA content measured by flow cytometry of Sytox Green labeled cells. Cells were synchronized in G1 by nitrogen starvation and released to 25°, 36°, and 0.01% MMS nitrogen-containing medium. WT (FY261), *mcm4-c106* (FY 4311). The indicated times correspond to the time after release. (C) Pulsed field gel electrophoresis (PFGE) analysis in each genotype in untreated asynchronous (AS) cells, after 4 hr 36° (4 hr) and after 2hr release to 25° (R). WT (FY 528), *mcm4-M68* (FY784), and *mcm4-c106* (FY 4311). *S. pombe* chromosomes are indicated on the left. (D) Relative viability of cultures during incubation with 0.01% MMS. The indicated cultures were plated at 25° on YES plates and the viability was compared to the starting culture. MMS, methyl methanesulfonate; WT, wild-type; YES, yeast extract + supplements.

We observed no evident Chk1 phosphorylation in asynchronously growing cultures at 25° in the absence of treatment (Figure 4, A and B). Despite this, we found that double mutants between the *mcm4-c106* and either *rad3Δ* or *chk1Δ* were inviable. However, double mutants with the S phase checkpoint mutant *cds1Δ* were viable (Table 2). We conclude that, even though we do not observe shifted mobility of Chk1 at permissive temperature, there is sufficient stress even in unperturbed *mcm4-c106* cells to cause them to depend upon the damage checkpoint for viability.

Repair foci accumulate in mcm4-c106

Previously, we examined replication stress by examining the accumulation of repair foci corresponding to the single strand DNA binding protein RPA (labeled with CFP), or the recombination protein Rad52 (labeled with YFP), and have observed differences in their distribution, pattern, and intensity in different conditions (Bailis *et al.* 2008; Sabatinos *et al.* 2012, 2015). There are dramatically different phenotypes between two different temperature-sensitive alleles. *mcm4-M68* forms multiple small foci and robustly arrests division at permissive temperature, while *mcm4-dg* forms a single large megafocus and undergoes continued division (Bailis *et al.* 2008; Sabatinos *et al.* 2015). Therefore, we examined repair foci fluorescence in both wild-type and *mcm4-c106* cells either shifted or released from 36°, or from MMS (Figure 5).

At 25°, *mcm4-c106* shows a modest increase in cells with both foci compared to the wild type, consistent with an increased basal level of stress (Figure 5, A–C). Following a shift to 36°, *mcm4-c106* accumulated numerous small foci of RPA-CFP and Rad52-YFP and these remain after 2 hr of release, whereas the foci in wild-type cells decline by 4 hr at 36° (Figure 5, A–C) (Sabatinos *et al.* 2015). The *mcm4-c106* cells did not divide in the first 2 hr following release. This suggests multiple dispersed damage sites, similar to *mcm4-M68*.

In wild-type cells during a 4 hr treatment with 0.01% MMS or at 2 hr after release from MMS, there is modest increase in cells with RPA or Rad52 foci (Figure 5, A, D, and E). This increase is measured from approximately 20% in untreated cells to about 50% in treated cells, but

most of these have just one or two foci. In contrast, while *mcm4-c106* cells have similar overall levels of focus formation in untreated cells, up to 80% of the cells have at least one focus in treated cells, and a strikingly large fraction contains multiple bright signals, which persist through the period of release. The majority of the RPA foci observed overlap with Rad52 foci (Figure 5, A, D, and E). Therefore, there is evidence for constitutive repair foci in *mcm4-c106* cells and these are dramatically increased upon exposure to MMS.

rif1Δ rescues mcm4-c106 MMS phenotype

One response to replication stress is to activate dormant origins (reviewed in Alver *et al.* 2014). The *mcm6-S1* mutant, which affects another subunit of the MCM complex, is the only other MCM allele that displays MMS sensitivity (Maki *et al.* 2011). Deletion of the S-phase cyclin *cig2* rescues this sensitivity, presumably by delaying G1/S phase and allowing additional licensing of origins (Maki *et al.* 2011). Therefore, we examined a double mutant of *cig2Δ mcm4-c106*. In contrast to the results reported for *mcm6-S1*, we observed only a very slight suppression of MMS sensitivity (Figure S4).

Unexpectedly, a double mutant *rif1Δ mcm4-c106* showed a dramatic rescue of MMS sensitivity (Figure 6B). Rif1 has recently been identified as an antagonist of DDK kinase-mediated phosphorylation of MCM, and regulates timing of origin firing (Hayano *et al.* 2012; Yamazaki *et al.* 2013; Davé *et al.* 2014; Hiraga *et al.* 2014; Mattarocci *et al.* 2014). Despite this dramatic rescue of the MMS phenotype, however, *rif1Δ* does not rescue the temperature sensitivity of *mcm4-c106* (Figure 6A).

Mcm4-c106 requires fork protection complex for viability

There is a central replisome scaffold that links the leading and lagging strand polymerases and the MCM helicase, including Mcl1(ScCtf4), Mrc1, the fork protection complex (FPC) Swi1(ScTof1), and Swi3(ScCsm3) (reviewed in Aze *et al.* 2013; Leman and Noguchi 2012; Errico and Costanzo 2012). Mutants defective in these nonessential proteins are all sensitive to MMS, indicating that robust coupling of the helicase and polymerase is required for proper response to
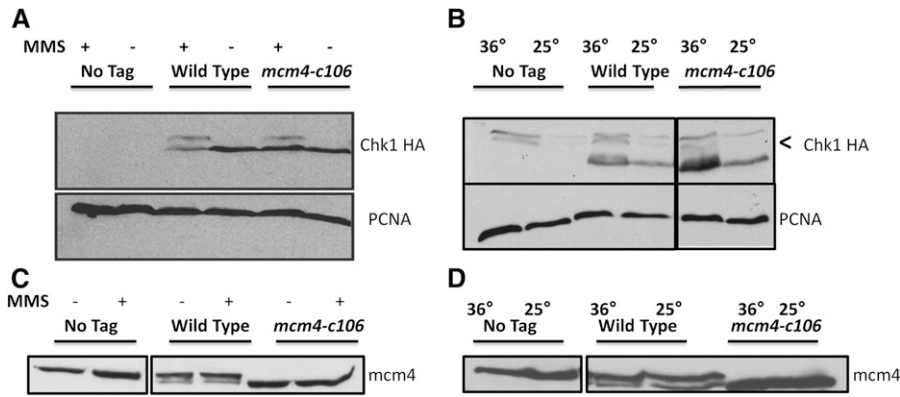
Figure 4 Mcm4 protein levels and Chk1 phosphorylation in response to MMS and 36°. (A) Evidence for Chk1 activation following 0.01% MMS for 4 hr. Chk1 mobility in SDS-PAGE was used as a proxy for phosphorylation. Lanes 1 and 2, *mcm4-c106* (FY 4311); lanes 3 and 4, *chk1-HA* (FY 4611); lanes 5 and 6 *mcm4-c106 chk1-HA* (FY6281). Arrow indicates phosphoshift. (B) Activation of Chk1 following 4 hr incubation at 36°. Lanes 1 and 2, *mcm4-c106* (FY 4311); lanes 3 and 4, *chk1-HA* (FY 4611); lanes 5 and 6, *mcm4-c106 chk1HA* (FY6281). (C) Mcm4 protein levels following MMS treatment. (D) Mcm4 protein levels following incubation at 36°. MMS, methyl methanesulfonate; PCNA, proliferating cell nuclear antigen.

alkylation stress. We observed that, similar to *mcm4-c106*, the MMS sensitivity associated with *swi1Δ* and *swi3Δ* is suppressed in *rif1Δ* double mutants (Figure 6C and Table 2), suggesting a related function for the C-terminus and Swi1 and Swi3. Therefore, we tested epistasis between *mcm4-c106* and FPC components. We found that double mutants between *mcm4-c106* and *swi1Δ*, *swi3Δ*, or *mrc1Δ* are all inviable, even at 25°. Deletion of *rif1Δ* did not rescue the inviability of *swi1Δ mcm4-c106* or *swi3Δ mcm4-c106* strains. A double mutant between the *mcl1-1* temperature-sensitive strain (Sc CTF4) (Williams and McIntosh 2002) and *mcm4-c106* was isolated, but grew so poorly that it was impossible to assess its MMS sensitivity (Table 2).

The DDK kinase Hsk1 (ScCdc7) is essential for DNA replication, in part due to its phosphorylation of MCM proteins (Masai *et al.* 2000, 2006; Sheu and Stillman 2006). It also interacts with the fork protection complex (Sommariva *et al.* 2005; Matsumoto *et al.* 2005) and antagonizes Rif1 (Hayano *et al.* 2012; Davé *et al.* 2014). Previously, we showed that the temperature-sensitive mutant *hsk1-1312* is sensitive to MMS and that wild-type Hsk1/DDK persists on the chromatin during MMS treatment, which depends upon the regulatory subunit Dfp1 (Dolan *et al.* 2010). Consistent with Hsk1 working in concert with FPC, we observed that the double mutants of *mcm4-c106 hsk1 1312* and *mcm4-c106 dfp-r35* formed microcolonies that could not be propagated. Thus, FPC and Hsk1, which are important for the MMS response, are also essential in the absence of the Mcm4 C-terminus.

The Ctf18 protein is part of an alternative replication factor C complex RFC clamp loader (Mayer *et al.* 2001; Hanna *et al.* 2001) that is associated with DNA polε (García-Rodríguez *et al.* 2015). In budding yeast and humans, Ctf18 associates with two additional subunits, Dcc1 and Ctf8, to form a heptameric complex that has been shown to have a role in sister chromatid cohesion (Mayer *et al.* 2001; Xu *et al.* 2007; Gellon *et al.* 2011) and a role in facilitating genomic stability (Gellon *et al.* 2011); this complex is also required for the replication checkpoint (Kubota *et al.* 2011). Additionally, in fission yeast, *ctf18Δ* is lethal with *swi1Δ* and *swi3Δ* (Ansbach *et al.* 2008). We find that double mutants *mcm4-c106 ctf18Δ* and *mcm4-c106 ctf8Δ* are viable, but with a modestly reduced permissive temperature (32°) (Figure 7A). They show a little change in MMS sensitivity relative to their parents (Figure 7B and Table 2). This suggests that the Ctf18 complex may be part of a common epistasis group with the Mcm4 C-terminus.

Chl1 is a helicase linked to the lagging strand that is a high copy suppressor of *swi1Δ* damage sensitivity (Ansbach *et al.* 2008), and it further has a role in sister chromatid cohesion in mitosis (Petronczki

et al. 2004). *chl1Δ* is lethal when combined with *ctf18Δ* (Ansbach *et al.* 2008). Double mutants with *mcm4-c106* and *chl1Δ* show increased sensitivity to MMS compared to their parents, but no effects on temperature (Figure 7C).

S. pombe Swi1 and Swi3, Ctf18 complex, and Hsk1 have all been linked to defects in chromosome cohesion (Bailis *et al.* 2003; Ansbach *et al.* 2008; Rapp *et al.* 2010). A temperature-sensitive mutation affecting the cohesin subunit *rad21-K1* combined with *ctf18Δ* shows increased sensitivity to MMS compared to the parents (Ansbach *et al.* 2008). Therefore, we examined a double mutant *mcm4-c106 rad21-K1*. This strain is viable and shows a similar MMS sensitivity to the parent *rad21-K1* (Figure 7D), suggesting that Rad21 also falls in an epistasis group with the Mcm4 C-terminus.

We tested several other mutations affecting proteins associated with the core replisome. Both temperature-sensitive mutations *cdc20-M10* and *pol1-1*, encoding the leading strand DNA polymerase ε (D'Urso and Nurse 1997) and polymerase α (D'Urso *et al.* 1995), respectively, were viable in combination with *mcm4-c106*, while a temperature-sensitive allele *cdc6-23* affecting the lagging strand DNA polymerase δ (Iino and Yamamoto 1997) is lethal (data not shown).

Mcm4-c106 interactions with repair pathways

Finally, we examined genetic interactions with other mutants in the MMS response pathway. The post replication repair (PRR) pathway includes both error free and error prone branches that facilitate the bypass of base lesions (reviewed in Huang and D'Andrea 2006; Ulrich and Walden 2010). These are regulated by levels of ubiquitylation on PCNA (Frampton 2006). We examined double mutants of *mcm4-c106* with repair mutants *mms2Δ*, *ubc13Δ*, *pcn1-K164R*, and *rad8Δ*. The double mutants were significantly more MMS sensitive than either single mutant, consistent with the mutants working in different pathways. None of these mutants showed a growth defect in the absence of MMS (Figure S5A). Double mutant error prone polymerases *rev3Δ*, *rev1Δ*, *polκΔ*, or *eso1-Δ eta* (Figure S5B) were all more sensitive than the single TLS mutant parents. Interestingly, while the double mutants with *polk* or *rev1Δ* were more sensitive than *mcm4-c106*, double mutants with *eso1-Δ eta* or *rev3Δ* were slightly less sensitive. The basis for this difference is unknown.

Effects of mcm4-c106 in recombination defective mutants

Replication fork stability and fork restart depend on proteins associated with recombination (reviewed in Lambert and Carr 2013; Neelsen and

■ Table 2 Sensitivity to MMS of double mutants of genes involved in different aspects of the cell cycle

Category	Mutant	Function	Phenotype with c106[a]	MMS Phenotype[b]
Checkpoint	cds1Δ	Kinase; S phase/replication checkpoint	Viable	>mcm4-c106
Checkpoint	chk1Δ	Kinase; G2/damage checkpoint	Synthetic lethal	ND
Checkpoint	mad2Δ	Spindle checkpoint	Viable	=mcm4-c106
Checkpoint	rad26Δ	Checkpoint protein	Synthetic lethal	ND
Checkpoint	rad3Δ	Kinase	Synthetic lethal	ND
Cohesion	chl1Δ	Helicase	Viable	> mcm4-c106
Cohesion	rad21-K1	Cohesin protein	Viable	= rad21-K1
Replication	mcl1-1 ts	Part of the FPC/cohesion	Sick	ND
Replication-FPC	mrc1Δ	Replication mutants/FPC	Synthetic lethal	ND
Replication-FPC	swi1Δ	Replication mutants/FPC	Synthetic lethal	ND
Replication-FPC	swi3Δ	Replication mutants/FPC	Synthetic lethal	ND
Replication	hsk1-1312	DDK kinase	Synthetic lethal	ND
Replication	dfp1-r35	DDK kinase	Viable/sick	ND
Replication, genome stability	rif1Δ	Rif1 antagonist of DDK	Viable	rescued
Genome stability	brc1Δ	Genome stability	Viable	mcm4-c106
Replication clamp loader	ctf8Δ	Cohesion-specific clamp loader	Viable < temp	= mcm4-c106
Replication clamp loader	ctf18Δ	Cohesion-specific clamp loader	Viable < temp	= mcm4-c106
Genome stability	fml1Δ	Helicase; genome stability	Viable	=fml1Δ
Genome stability	mus81Δ	Holiday junction resolvase	Sick	=mus81
Genome stability	rqh1Δ	Helicase; recombination antagonist	Viable	> mcm4-c106
Genome stability	srs2Δ	Helicase; recombination regulator	Viable	>mcm4-c106
Repair	eso1-Δeta	Eso1- Polη fusion; deletes polymerase domain. Error prone repair	Viable	≤mcm4c106
Repair	exo1Δ	Exonuclease I	Viable	= exo1Δ
Repair	mms2Δ	Ubiquitin ligase; error free repair	Viable	> mms2Δ
Repair	pcn1-K164R	PCNA; ubiquitin site mutant	Viable	= pcn1-K164R
Repair	polkΔ	Polκ; error prone repair	Viable	>mcm4-c106
Repair	rad51Δ	Homologous recombination	Viable	=rad51Δ
Repair	rad8Δ	Ubiquitin ligase-helicase; error free repair	Viable	>rad8Δ
Repair	rev1Δ	Deoxycytidyl transferase; error prone repair	Viable	≥ mcm4-c106
Repair	rev3Δ	Polζ Error prone repair	Viable	<mcm4-c106
Repair	rhp18Δ	PCNA ubiquitin ligase	Viable	= rhp18Δ
Repair	ubc13Δ	Ubiquitin ligase; error free	Viable	> ubc13Δ
Repair	chp1Δ	Heterochromatin protein	Viable	=mcm4-c106
Repair	cig2Δ/_cyc17	S phase cyclin	Viable	≤ mcm4-c106
Repair	reb1Δ	Transcription termination	Viable < temp	=mcm4-c106
Repair	swi6Δ	Heterochromatin protein	Viable	= mcm4-c106
	rad22Δ		Viable/slow growing	ND
	cdc20- M10(polε)		Viable	ND
	cdc6- 23(polδ)		Synthetic lethal	NA
	psf2ts	Component of the GINS replication complex	Viable	>mcm4-c106
	pol1-1(polα)		Viable	ND
	rad50Δ		Synthetic lethal	NA

Double mutant phenotypes between *mcm4-c106* and other mutants in the indicated classes. MMS, methyl methanesulfonate; ND, Not Determined; FPC, fork protection complex; DDK, Dbf4-dependent kinase; PCNA, proliferating cell nuclear antigen; NA, Not Applicable.

[a] Phenotype: viable means no change in temperature sensitivity. Synthetic lethal is dead at temperatures. Sick shows reduced growth rate at all temperatures. <temp has reduced maximum growth temperature.

[b] MMS phenotype is determined relative to the most sensitive parent (indicated) being > (greater sensitivity), < (less sensitive), or = (equal sensitivity).
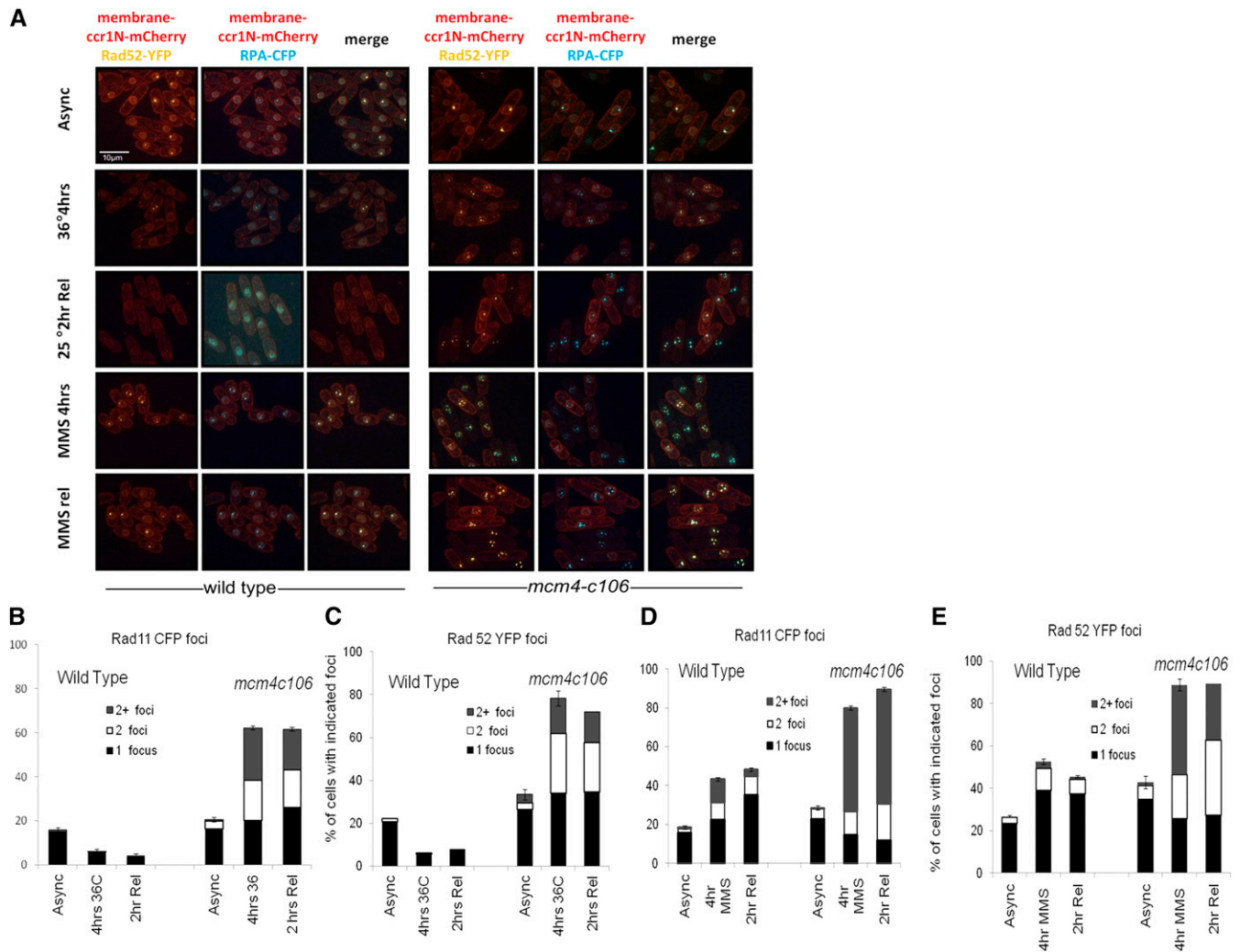
Figure 5 Accumulation of repair foci in *mcm4-c106* in response to MMS and temperature. (A) Membrane (ccr1N-mCherry), RPA-CFP (blue), and Rad52-YFP (yellow) focus patterns during treatment at restrictive temperature (36°) and release. Multiple small foci were observed with the *mcm4-c106* that remained after release. RPA and Rad52 focus patterns during treatment with 0.01% MMS for 4 hr and release for 2 hr. Multiple small foci were observed during treatment and release in the *mcm4-c106* compared to the wild type. Scale 10 μm. (B) Quantification of Rad11 foci of wild-type and *mcm4-c106* during 36° treatment and release. (C) Quantification of Rad52 foci of wild-type and *mcm4-c106* during 36° treatment and release. (D) Quantification of Rad11 foci of wild-type and *mcm4-c106* during 4 hr MMS treatment and release. (E) Quantification of Rad52 foci of wild-type and *mcm4-c106* during 4 hr MMS treatment and release. Two or more independent experiments were pooled and a 95% C.I. was calculated. Async, asynchronous; MMS, methyl methanesulfonate.

Lopes 2015). We constructed double mutants between *mcm4-c106* and mutations that disrupt recombinational repair of damaged forks including: *mus81Δ* (endonuclease; Boddy *et al.* 2001), *rad50Δ* (MRN complex; Bressan *et al.* 1999), *rad51Δ* (homologous recombination regulator; Muris *et al.* 1993), *rqh1Δ* (RecQ helicase; Stewart *et al.* 1997), and *srs2Δ* (helicase; Wang *et al.* 2001; Maftahi *et al.* 2002). We find that *rad50Δ mcm4-c106* is synthetic lethal, indicating that the constitutive damage of *mcm4-c106* requires an active MRN complex for survival. The *mus81Δ* double mutant had an extreme growth defect even at 25°, with slow growth and elongated cell morphology, suggesting the formation of structures that require Mus81 for successful resolution. In contrast, *rad51Δ*, *rqh1Δ*, or *srs2Δ* double mutants showed no growth defects at permissive temperature, but were sensitive to MMS at a level similar or greater than the most sensitive parent (Figure S6, A and B). These data suggest that these proteins function in a pathway separate from the C-terminus of Mcm4.

DISCUSSION

Fission yeast Mcm4 is an essential subunit of the MCM helicase, which is a critical component in the response to replication stress. Previous studies have shown that the Mcm4 C-terminal domain (CTD) is important for the efficient recovery of HU-stalled replication forks, and a C-terminal truncation *mcm4-c84* causes excessive formation of ssDNA when replication is inhibited by hydroxyurea (Nitani *et al.* 2008). That study also identified a larger CTD truncation mutant, *mcm4-c106*, as HU-sensitive and temperature-sensitive, but did not characterize it further.

Our initial examination of the temperature-sensitive phenotype of *mcm4-c106* shows three distinct phenotypes that we characterized. First, their temperature-sensitive phenotype has important differences from those in other alleles of *mcm4+*. Second, they are MMS-sensitive. Finally, they have distinct replication defects at permissive temperature, including a novel spectrum of genetic interactions
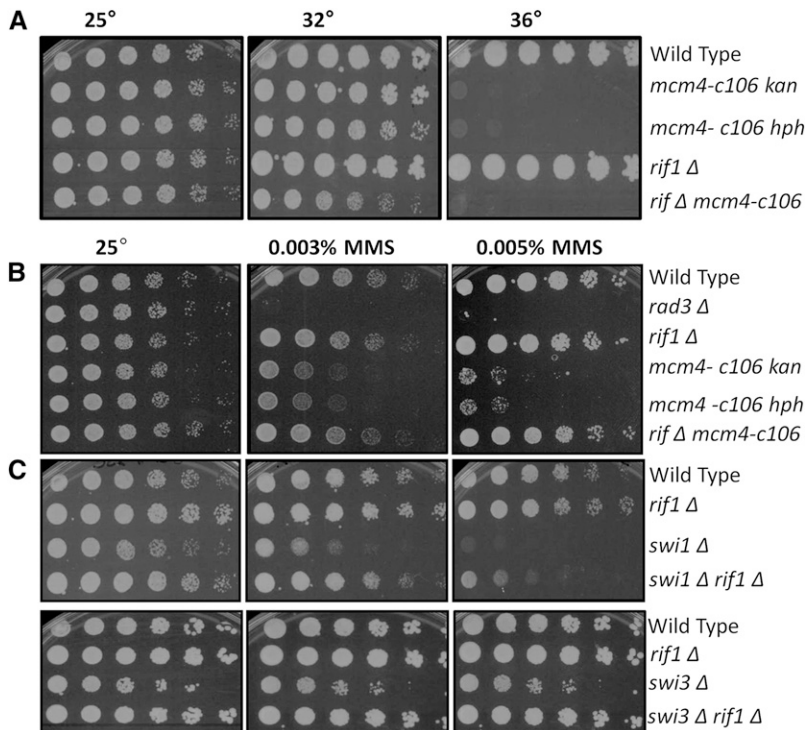
Figure 6 rif1Δ rescues the mcm4-c106 MMS phenotype. (A) Temperature sensitivity evaluated by strains grown overnight at 25°, 1:5 serially diluted, and plated on YES (rich media) at 25° as control, and 32° and 36° to observe the temperature effect. (B) and (C) MMS sensitivity evaluated by strains grown overnight at 25°, 1:5 serially diluted, and plated on YES (rich media) as control, and 0.003% and 0.005% MMS at 25°. MMS, methyl methanesulfonate; YES, yeast extract + supplements.

Similar to the original mcm4-M68 strain (Bailis et al. 2008; Sabatinos et al. 2015), we observe that mcm4-c106 cells accumulate a 2C DNA content at restrictive temperature, indicating substantial bulk DNA synthesis (Figure 3B). Cells elongate and do not divide, demonstrating successful activation of the checkpoint, confirmed by a phosphorylation-induced shift of the Chk1 kinase (Figure 4B). The cells also show increased RPA and Rad52 foci during normal growth, temperature shift, and following release, with small punctate morphology similar to that observed in mcm4-M68 (Figure 5A; Sabatinos et al. 2015). Strikingly, however, mcm4-c106 chromosomes enter a pulsed-field gel normally, both at restrictive temperature and following release, without the chromosome breaks and or structural intermediates that impair chromosome migration in mcm4-M68. We previously suggested that the breaks in mcm4-M68 reflect distinct structures targeted by the Mus81 nuclease; (Sabatinos et al. 2015) the intact chromosomes of mcm4-c106 suggest that whatever structures are formed at restrictive temperature are not the same. The temperature-sensitive phenotype may reflect either Mcm4 protein unfolding (although the protein remains detectable) or some intrinsically temperature-sensitive activity involved in replisome coupling that renders the C-terminus essential at high temperatures. In any case, some fractions of the cells are competent to restart the cell cycle, indicating that the damage they suffer is not irreversible and that the MCM complex remains largely intact and located correctly in the nucleus, which is not seen for mcm4-M68 (Pasion and Forsburg 1999).

In contrast to the original mcm4-M68 allele, the mcm4-c106 cells have clear deficiencies even under permissive conditions. Efficiency of plasmid transformation is a metric for replication efficiency (Clyne and Kelly 1997; Tye 1999), and we observe a substantial reduction in plasmid transformation efficiency and colony size, consistent with a defect in replication in mcm4-c106 but not in mcm4-M68 at 25°. In addition, the mcm4-c106 cells are synthetically lethal with rad3Δ or chk1Δ checkpoint kinase mutants, and have an increased level of RPA and Rad52 foci at permissive temperature, which suggests that the cells suffer some form of constitutive DNA damage present even at 25°. This is not observed in mcm4-M68. We also found synthetic lethality between mcm4-c106 MRN component rad50Δ, and severe synthetic sickness with mus81Δ, which implicates fork processing and restart in the recovery from innate stress. The absence of a synthetic phenotype associated with rad51Δ suggests that typical homologous recombination mechanisms are not required.

Interestingly, we found that mcm4-c106 is also sensitive to alkylation damage caused by MMS treatment at the permissive temperature, unlike other mcm4 alleles (Figure 1B). Previously, the only MMS-sensitive MCM identified was an allele of mcm6 (mcm6-S1) that is defective in pre-RC assembly (Maki et al. 2011). Because mcm4-c106 cells showed increased sensitivity to MMS in combination with mutations that directly affect downstream repair, including homologous recombination, error free, and error prone postreplication repair pathways, we propose that its defect is not in repair but in fork stability, or restart by template switching.

MMS sensitivity has been observed in mutants affecting a subset of additional replisome components including the fork protection complex (swi1Δ, swi3Δ, and mrc1Δ), scaffolding protein mcl1, and the DDK kinase subunits hsk1-1312 or dfp1-r35 (Fung et al. 2002; Williams and McIntosh 2002; Sommariva et al. 2005; Dolan et al. 2010). MMS treatment in fission yeast results in slowing of the replication fork (Chahwan et al. 2003; Kumar and Huberman 2004; Willis and Rhind 2009). Although there have been reports that MMS generates DNA double strand breaks (Wyatt and Pittman 2006), this breakage is likely be an artifact of the procedure used to extract DNA (Lundin et al. 2005), so the PFGE results are likely uninformative. Rather, a major form of recovery is fork arrest, template switching, and repriming (reviewed in Branzei and Foiani 2010), which leads to accumulation of single-stranded DNA and increased recombination intermediates (Willis and Rhind 2009; Koulintchenko et al. 2012). Formation of these MMS recombination structures is disrupted in swi1Δ and swi3Δ, and also in rad2Δ mutants lacking the FEN1 flap endonuclease (Noguchi et al. 2004; Koulintchenko et al. 2012). In budding yeast, DNA
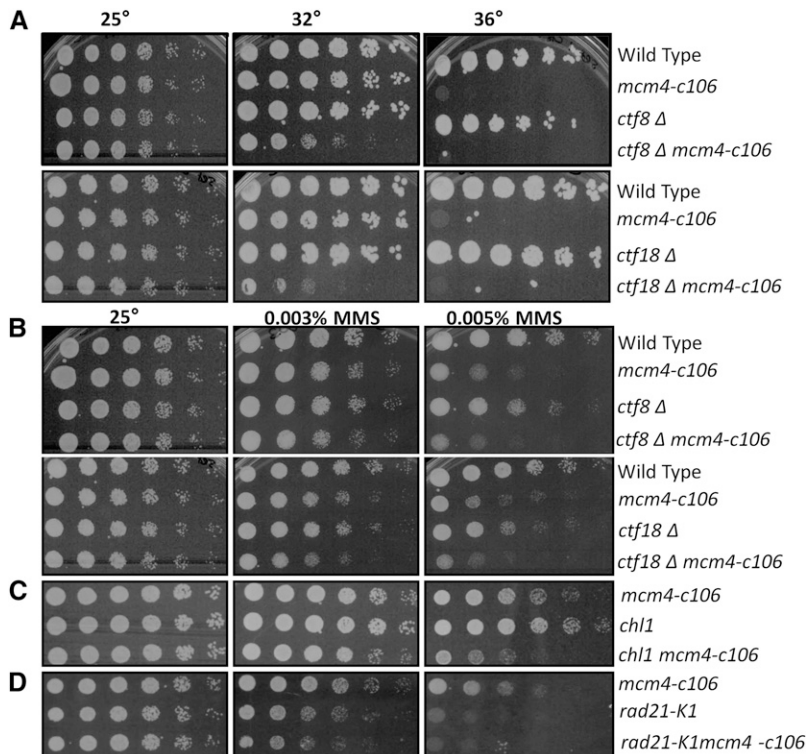
Figure 7 *mcm4-c106* interactions with alternative replication factor C (RFC). (A) *mcm4-c106* combined with RFC^Ctf18^Δ and RFC^Ctf8^Δ. Representative response to temperature was assayed by serial dilutions. Strains were grown overnight at 25°, 1:5 serially diluted, and plated on YES (rich media) as the control, and 32° and 36° to observe the temperature effect. (B) Representative response to MMS assessed by serial diluted samples plated on the indicated concentrations of MMS. (C) *chl1Δ mcm4-c106* and (D) cohesion subunit *rad21-K1 mcm4-c106* effects on MMS. MMS, methyl methanesulfonate; YES, yeast extract + supplements.

polymerase α and the Mcl1 ortholog Ctf4 are required for template switching, and evidence indicates that this requirement is not limited to lagging strand lesions (Fumasoni *et al.* 2015). These observations suggest that the scaffolding proteins that link CMG and polymerases are key players to allow successful template switching. The sensitivity of *Mcm4-c106* is unlikely to reflect disruptions in the scaffold itself, as models of CMG suggest that Mcm4 lies on the ring face opposite to Cdc45, GINS, Ctf4, and polymerases (O'Donnell and Li 2016).

We found that *rif1Δ* rescues the MMS sensitivity of *mcm4-c106*, but not its temperature sensitivity. *rif1Δ* also rescues the MMS sensitivity of *swi1Δ* or *swi3Δ*. Rif1 in budding yeast has a role in replication timing, via the recruitment of Glc7 phosphatase (Hayano *et al.* 2012; Davé *et al.* 2014; Mattarocci *et al.* 2014; Hiraga *et al.* 2014; Peace *et al.* 2014). This antagonizes the DDK-mediated phosphorylation of Mcm4 that activates replication. Intriguingly, Rif1 is also proposed to modify the response to ssDNA that activates the checkpoint (Xu *et al.* 2010), as well as contributing to resection in break repair (Martina *et al.* 2014). A new study also links Rif1 to resolution of chromosome entanglements (Zaaijer *et al.* 2016). In fission yeast, *rif1Δ* rescues temperature sensitivity of *hsk1-89* (Hayano *et al.* 2012; Davé *et al.* 2014) and *hsk1-1312* (J. P. Yuan and S. L. Forsburg, unpublished data). However, Rif1 is not essential for cellular responses to replication stress (Hayano *et al.* 2012; Peace *et al.* 2014).

There are several models by which this rescue could occur. One way would be by activating otherwise dormant origins, as *rif1Δ* is proposed to deregulate origin timing by antagonizing DDK (Hayano *et al.* 2012). Origin activation has been proposed to rescue the MMS sensitivity of *mcm6-S1*, another MCM subunit (Maki *et al.* 2011). However, unlike *mcm6-S1*, the MMS sensitivity of *mcm4-c106* was not notably rescued by deletion of the S phase cyclin *cig2*, suggesting that additional pre-RC formation is not a mechanism for rescue. Alternatively, rescue may be linked to Rif1 antagonism of the Hsk1/DDK kinase, which is localized to the chromatin in MMS and potentially recruited by the FPC (Sommariva *et al.* 2005; Matsumoto *et al.* 2005; Dolan *et al.* 2010). Hsk1

is known to phosphorylate Mrc1 (associated with FPC) and the checkpoint clamp Rad9 during replication stress (Matsumoto *et al.* 2010; Furuya *et al.* 2010). In the absence of FPC, therefore, loss of localized Hsk1 activity may be balanced by the absence of the Rif1 antagonist.

The similarity of rescue of the MMS phenotype of *mcm4-c106* and *swi1Δ* or *swi3Δ* led us to investigate whether they are in a common epistasis group. Contrary to that model, we observed synthetic lethality between *mcm4-c106* and FPC mutants *swi1Δ*, *swi3Δ*, and *mrc1Δ*, as well as DDK mutants *hsk1-1312* and *dfp1-r35*, indicating that an intact fork-protection complex including DDK must be present in the absence of the Mcm4 C-terminus. A similar synthetic lethal phenotype with the FPC was not observed with *mcm4-c84*, which harbors a shorter truncation of the C-terminus (Nitani *et al.* 2008), so this is unlikely to be related to the HU-ssDNA phenotype observed in that study.

Because we see no phenotype in double mutants with the replication checkpoint kinase *cds1Δ*, we conclude that this synthetic lethality is not related to the S phase checkpoint activation by FPC (Noguchi *et al.* 2003), but rather to the FPC's structural role linking the helicase to the polymerase (Noguchi *et al.* 2004; Lou *et al.* 2008; reviewed in Aze *et al.* 2013).

Mcl1 (ScCtf4) links the helicase to the lagging strand through the interaction with polymerase α and direct interaction with the GINS subcomplex (Gambus *et al.* 2009; Simon *et al.* 2014). At least one arm of the helicase coupling system is required for viability, because *mcl1-1 swi1Δ* double mutants are synthetically lethal (J. P. Yuan and S. L. Forsburg, unpublished results). Therefore, one possibility is that mutation of *mcm4-c106* may lead to defects in coupling to the lagging strand side of the replisome, making it dependent upon the FPC and the leading strand coupling for viability even at permissive temperature.

FPC mutants are also synthetically lethal, with mutations affecting Ctf18 and Ctf8 forming an alternative RFC clamp loader complex (Ansbach *et al.* 2008). Long linked to sister chromatid cohesion (Hanna *et al.* 2001; Mayer *et al.* 2001), Ctf18 has more recently been associated with DNA damage response and replication checkpoint

activation (Crabbé *et al.* 2010; Kubota *et al.* 2011). We observed modestly reduced permissive temperature in *ctf18Δ mcm4-c106*, but no defect at permissive temperature and little change in MMS sensitivity, which suggests that they are in a common epistasis group at this temperature. Double mutants between *mcm4-c106* and the *mcl1-1* temperature-sensitive allele were viable, although significantly sicker than either parent. Our genetic analysis offers further tantalizing evidence that this phenotype may be linked to cohesion. FPC, Mcl1, polε, DDK, and Ctf18 are all associated with sister chromatid cohesion in *S. pombe* and other systems (Hanna *et al.* 2001; Williams and McIntosh 2002; Bailis *et al.* 2003; Edwards *et al.* 2003; Xu *et al.* 2007; Ansbach *et al.* 2008; Rapp *et al.* 2010). We observed no evidence for chromosome segregation errors in *mcm4-c106* that would indicate a sister chromatid cohesion defect. A temperature-sensitive mutation affecting the cohesin subunit *rad21-K1* is synthetic lethal with either *swi1Δ* (Ansbach *et al.* 2008; Dolan *et al.* 2010) or *hsk1-1312* (Snaith *et al.* 2000). In contrast to the substantial genetic interactions in other double mutants, we did not observe growth defects in *rad21-K1 mcm4-c106*. Additionally, the MMS sensitivity of *rad21 mcm4-c106* is similar to that of the *rad21-K1* parent. We propose that the C-terminus of Mcm4 may facilitate the recruitment of cohesin to promote a distinct fork maintenance or restart function.

As its name implies, the *S. pombe* cohesin *rad21* gene was first identified by its repair defect (Birkenbihl and Subramani 1992). Mutations in *rad21* are MMS-sensitive, and lie in an epistatic pathway with *rad50* (Hartsuiker *et al.* 2001). More recently, studies suggest that cohesin may influence replication origin activity by affecting 3-D genome organization (Guillou *et al.* 2010; Yun *et al.* 2016). Cohesin has been shown to be required for efficient template switching in budding yeast in a pathway that includes Ctf4 (*Sp* Mcl1) (Fumasoni *et al.* 2015). Particularly intriguing, Mcm4 has also been identified as a binding partner of mammalian Rad21 in two separate proteomics studies (Guillou *et al.* 2010; Panigrahi *et al.* 2012). We suggest that the extended C-terminus of Mcm4 collaborates with cohesin to promote fork stability during replication stress.

Together, these results indicate that *mcm4-c106* has a novel replication defect, likely to do with replisome uncoupling, that is distinct from that in other *mcm4* conditional alleles. Along with our previous study (Sabatinos *et al.* 2015), this suggests that physiological inspection of conditional mutant phenotypes is likely to identify new domains and interactions that assemble and maintain the replicative helicase.

ACKNOWLEDGMENTS

LITERATURE CITED

Abid Ali, F., and A. Costa, 2015 The MCM Helicase Motor of the Eukaryotic Replisome. J. Mol. Biol. 428: 1822–1832.

Alver, R. C., G. S. Chadha, and J. J. Blow, 2014 The contribution of dormant origins to genome stability: from cell biology to human genetics. DNA Repair (Amst.) 19: 182–189.

Ansbach, A. B., C. Noguchi, I. W. Klansek, M. Heidlebaugh, T. M. Nakamura *et al.*, 2008 RFCCtf18 and the Swi1-Swi3 complex function in separate and redundant pathways required for the stabilization of replication forks to facilitate sister chromatid cohesion in Schizosaccharomyces pombe. Mol. Biol. Cell 19: 595–607.

Aze, A., J. C. Zhou, A. Costa, and V. Costanzo, 2013 DNA replication and homologous recombination factors: acting together to maintain genome stability. Chromosoma 122: 401–413.

Bagley, B. N., T. M. Keane, V. I. Maklakova, J. G. Marshall, R. A. Lester *et al.*, 2012 A dominantly acting murine allele of Mcm4 causes chromosomal abnormalities and promotes tumorigenesis. PLoS Genet. 8: e1003034.

Bailis, J. M., P. Bernard, R. Antonelli, R. C. Allshire, and S. L. Forsburg, 2003 Hsk1-Dfp1 is required for heterochromatin-mediated cohesion at centromeres. Nat. Cell Biol. 5: 1111–1116.

Bailis, J. M., D. D. Luche, T. Hunter, and S. L. Forsburg, 2008 Minichromosome maintenance proteins interact with checkpoint and recombination proteins to promote s-phase genome stability. Mol. Cell. Biol. 28: 1724–1738.

Barbet, N., W. J. Muriel, and A. M. Carr, 1992 Versatile shuttle vectors and genomic libraries for use with Schizosaccharomyces pombe. Gene 114: 59–66.

Birkenbihl, R. P., and S. Subramani, 1992 Cloning and characterization of rad21 an essential gene of Schizosaccharomyces pombe involved in DNA double-strand-break repair. Nucleic Acids Res. 20: 6605–6611.

Boddy, M. N., P. H. Gaillard, W. H. McDonald, P. Shanahan, J. R. Yates *et al.*, 2001 Mus81-Eme1 are essential components of a Holliday junction resolvase. Cell 107: 537–548.

Branzei, D., and M. Foiani, 2010 Maintaining genome stability at the replication fork. Nat. Rev. Mol. Cell Biol. 11: 208–219.

Bressan, D. A., B. K. Baxter, and J. H. Petrini, 1999 The Mre11-Rad50-Xrs2 protein complex facilitates homologous recombination-based double-strand break repair in Saccharomyces cerevisiae. Mol. Cell. Biol. 19: 7681–7687.

Brun, C., D. D. Dubey, and J. A. Huberman, 1995 pDblet, a stable autonomously replicating shuttle vector for Schizosaccharomyces pombe. Gene 164: 173–177.

Chahwan, C., T. M. Nakamura, S. Sivakumar, P. Russell, and N. Rhind, 2003 The fission yeast Rad32 (Mre11)-Rad50-Nbs1 complex is required for the S-phase DNA damage checkpoint. Mol. Cell. Biol. 23: 6564–6573.

Clyne, R. K., and T. J. Kelly, 1997 Identification of autonomously replicating sequence (ARS) elements in eukaryotic cells. Methods 13: 221–233.

Costa, A., I. Ilves, N. Tamberg, T. Petojevic, E. Nogales *et al.*, 2011 The structural basis for MCM2–7 helicase activation by GINS and Cdc45. Nat. Struct. Mol. Biol. 18: 471–477.

Costa, A., L. Renault, P. Swuec, T. Petojevic, J. J. Pesavento *et al.*, 2014 DNA binding polarity, dimerization, and ATPase ring remodeling in the CMG helicase of the eukaryotic replisome. eLife 3: e03273.

Coxon, A., K. Maundrell, and S. E. Kearsey, 1992 Fission yeast cdc2l + belongs to a family of proteins involved in an early step of chromosome replication. Nucleic Acids Res. 20: 5571–5577.

Crabbé, L., A. Thomas, V. Pantesco, J. De Vos, P. Pasero *et al.*, 2010 Analysis of replication profiles reveals key role of RFC-Ctf18 in yeast replication stress response. Nat. Struct. Mol. Biol. 17: 1391–1397.

Davé, A., C. Cooley, M. Garg, and A. Bianchi, 2014 Protein Phosphatase 1 Recruitment by Rif1 Regulates DNA Replication Origin Firing by Counteracting DDK Activity. Cell Reports 7: 53–61.

Devault, A., E. Gueydon, and E. Schwob, 2008 Interplay between S-Cyclin-dependent Kinase and Dbf4-dependent Kinase in Controlling DNA Replication through Phosphorylation of Yeast Mcm4 N-Terminal Domain. Mol. Biol. Cell 19: 2267–2277.

Ding, L., and S. L. Forsburg, 2014 Essential Domains of Schizosaccharomyces pombe Rad8 Required for DNA Damage Response. G3 (Bethesda) 4: 1373–1384.

Dolan, W. P., A. H. Le, H. Schmidt, J. P. Yuan, M. Green *et al.*, 2010 Fission yeast Hsk1 (Cdc7) kinase is required after replication initiation for induced mutagenesis and proper response to DNA alkylation damage. Genetics 185: 39–53.

D'Urso, G., and P. Nurse, 1997 Schizosaccharomyces pombe cdc20+ encodes DNA polymerase epsilon and is required for chromosomal replication but not for the S phase checkpoint. Proc. Natl. Acad. Sci. USA 94: 12491–12496.

D'Urso, G., B. Grallert, and P. Nurse, 1995 DNA polymerase alpha, a component of the replication initiation complex, is essential for the checkpoint coupling S phase to mitosis in fission yeast. J. Cell Sci. 108: 3109–18.

Edwards, S., C. M. Li, D. L. Levy, J. Brown, P. M. Snow *et al.*, 2003 Saccharomyces cerevisiae DNA polymerase epsilon and

polymerase sigma interact physically and functionally, suggesting a role for polymerase epsilon in sister chromatid cohesion. Mol. Cell. Biol. 23: 2733–2748.

Errico, A., and V. Costanzo, 2012 Mechanisms of replication fork protection: a safeguard for genome stability. Crit. Rev. Biochem. Mol. Biol. 47: 222–235.

Foiani, M., F. Marini, D. Gamba, G. Lucchini, and P. Plevani, 1994 The B subunit of the DNA polymerase alpha-primase complex in Saccharomyces cerevisiae executes an essential function at the initial stage of DNA replication. Mol. Cell. Biol. 14: 923–933.

Frampton, J., 2006 Postreplication Repair and PCNA Modification in Schizosaccharomyces pombe. Mol. Biol. Cell 17: 2976–2985.

Fumasoni, M., K. Zwicky, F. Vanoli, M. Lopes, and D. Branzei, 2015 Error-free DNA damage tolerance and sister chromatid proximity during DNA replication rely on the Polα/Primase/Ctf4 Complex. Mol. Cell 57: 812–823.

Fung, A. D., J. Ou, S. Bueler, and G. W. Brown, 2002 A conserved domain of Schizosaccharomyces pombe dfp1(+) is uniquely required for chromosome stability following alkylation damage during S phase. Mol. Cell. Biol. 22: 4477–4490.

Furuya, K., I. Miyabe, Y. Tsutsui, F. Paderi, N. Kakusho et al., 2010 DDK Phosphorylates checkpoint clamp component Rad9 and promotes its release from damaged chromatin. Mol. Cell 40: 606–618.

Gambus, A., F. van Deursen, D. Polychronopoulos, M. Foltman, R. C. Jones et al., 2009 A key role for Ctf4 in coupling the MCM2–7 helicase to DNA polymerase alpha within the eukaryotic replisome. EMBO J. 28: 2992–3004.

García-Rodríguez, L. J., G. De Piccoli, V. Marchesi, R. C. Jones, R. D. Edmondson et al., 2015 A conserved Polε binding module in Ctf18-RFC is required for S-phase checkpoint activation downstream of Mec1. Nucleic Acids Res. 43: 8830–8838.

Gellon, L., D. F. Razidlo, O. Gleeson, L. Verra, D. Schulz et al., 2011 New Functions of Ctf18-RFC in Preserving Genome Stability outside Its Role in Sister Chromatid Cohesion. PLoS Genet. 7: e1001298.

Gineau, L., C. Cognet, N. Kara, F. P. Lach, J. Dunne et al., 2012 Partial MCM4 deficiency in patients with growth retardation, adrenal insufficiency, and natural killer cell deficiency. J. Clin. Invest. 122: 821–832.

Green, M. D., S. A. Sabatinos, and S. L. Forsburg, 2015 Microscopy techniques to examine DNA replication in fission yeast. Methods Mol. Biol. 1300: 13–41.

Guillou, E., A. Ibarra, V. Coulon, J. Casado-Vela, D. Rico et al., 2010 Cohesin organizes chromatin loops at DNA replication factories. Genes Dev. 24: 2812–2822.

Hanna, J. S., E. S. Kroll, V. Lundblad, and F. A. Spencer, 2001 Saccharomyces cerevisiae CTF18 and CTF4 are required for sister chromatid cohesion. Mol. Cell. Biol. 21: 3144–3158.

Hartsuiker, E., E. Vaessen, A. M. Carr, and J. Kohli, 2001 Fission yeast Rad50 stimulates sister chromatid recombination and links cohesion with repair. EMBO J. 20: 6660–6671.

Hayano, M., Y. Kanoh, S. Matsumoto, C. Renard-Guillet, K. Shirahige et al., 2012 Rif1 is a global regulator of timing of replication origin firing in fission yeast. Genes Dev. 26: 137–150.

Hiraga, S. I., G. M. Alvino, F. Chang, H. Y. Lian, A. Sridhar et al., 2014 Rif1 controls DNA replication by directing Protein Phosphatase 1 to reverse Cdc7-mediated phosphorylation of the MCM complex. Genes Dev. 28: 372–383.

Huang, T. T., and A. D. D'Andrea, 2006 Regulation of DNA repair by ubiquitylation. Nat. Rev. Mol. Cell Biol. 7: 323–334.

Hughes, C. R., L. Guasti, E. Meimaridou, C.-H. Chuang, J. C. Schimenti et al., 2012 MCM4 mutation causes adrenal failure, short stature, and natural killer cell deficiency in humans. J. Clin. Invest. 122: 814–820.

Iino, Y., and M. Yamamoto, 1997 The Schizosaccharomyces pombe cdc6 gene encodes the catalytic subunit of DNA polymerase delta. Mol. Gen. Genet. 254: 93–97.

Ilves, I., T. Petojevic, J. J. Pesavento, and M. R. Botchan, 2010 Activation of the MCM2-7 helicase by association with Cdc45 and GINS proteins. Mol. Cell 37: 247–258.

Ishimi, Y., and D. Irie, 2015 G364R mutation of MCM4 detected in human skin cancer cells affects DNA helicase activity of MCM4 / 6 / 7 complex. J. Biochem. 157: 1–9.

Koulintchenko, M., S. Vengrova, T. Eydmann, P. Arumugam, and J. Z. Dalgaard, 2012 DNA Polymerase α (swi7) and the Flap Endonuclease Fen1 (rad2) Act Together in the S-Phase Alkylation Damage Response in S. pombe. PLoS One 7: e47091.

Kubota, T., S. Hiraga, K. Yamada, A. I. Lamond, and A. D. Donaldson, 2011 Quantitative Proteomic Analysis of Chromatin Reveals that Ctf18 Acts in the DNA Replication Checkpoint. Mol. Cell. Proteomics 10. Available at: http://www.mcponline.org/content/10/7/M110.005561.long.

Kumar, S., and J. A. Huberman, 2004 On the slowing of S phase in response to DNA damage in fission yeast. J. Biol. Chem. 279: 43574–43580.

Lambert, S., and A. M. Carr, 2013 Impediments to replication fork movement: stabilisation, reactivation and genome instability. Chromosoma 122: 33–45.

Langston, L. D., D. Zhang, O. Yurieva, R. E. Georgescu, J. Finkelstein et al., 2014 CMG helicase and DNA polymerase ε form a functional 15-subunit holoenzyme for eukaryotic leading-strand DNA replication. Proc. Natl. Acad. Sci. USA 111: 15390–15395.

Leman, A. R., and E. Noguchi, 2012 Local and global functions of Timeless and Tipin in replication fork protection. Cell Cycle 11: 3945–3955.

Liang, D. T., and S. L. Forsburg, 2001 Characterization of Schizosaccharomyces pombe mcm7(+) and cdc23(+) (MCM10) and interactions with replication checkpoints. Genetics 159: 471–486.

Liang, D. T., J. A. Hodson, and S. L. Forsburg, 1999 Reduced dosage of a single fission yeast MCM protein causes genetic instability and S phase delay. J. Cell Sci. 112: 559–67.

Lindner, K., J. Gregán, S. Montgomery, and S. E. Kearsey, 2002 Essential role of MCM proteins in premeiotic DNA replication. Mol. Biol. Cell 13: 435–444.

Liu, L. F., S. D. Desai, T. K. Li, Y. Mao, M. Sun et al., 2000 Mechanism of action of camptothecin. Ann. N. Y. Acad. Sci. 922: 1–10.

Lou, H., M. Komata, Y. Katou, Z. Guan, C. C. Reis et al., 2008 Mrc1 and DNA polymerase epsilon function together in linking DNA replication and the S phase checkpoint. Mol. Cell 32: 106–117.

Lundin, C., M. North, K. Erixon, K. Walters, D. Jenssen et al., 2005 Methyl methanesulfonate (MMS) produces heat-labile DNA damage but no detectable in vivo DNA double-strand breaks. Nucleic Acids Res. 33: 3799–3811.

Maftahi, M., J. C. Hope, L. Delgado-Cruzata, C. S. Han, and G. A. Freyer, 2002 The severe slow growth of Deltasrs2 Deltarqh1 in Schizosaccharomyces pombe is suppressed by loss of recombination and checkpoint genes. Nucleic Acids Res. 30: 4781–4792.

Maki, K., T. Inoue, A. Onaka, H. Hashizume, N. Somete et al., 2011 Abundance of prereplicative complexes (Pre-RCs) facilitates recombinational repair under replication stress in fission yeast. J. Biol. Chem. 286: 41701–41710.

Martina, M., D. Bonetti, M. Villa, G. Lucchini, and M. P. Longhese, 2014 Saccharomyces cerevisiae Rif1 cooperates with MRX-Sae2 in promoting DNA-end resection. EMBO Rep. 15: 695–704.

Masai, H., E. Matsui, Z. You, Y. Ishimi, K. Tamai et al., 2000 Human Cdc7-related kinase complex. In vitro phosphorylation of MCM by concerted actions of Cdks and Cdc7 and that of a critical threonine residue of Cdc7 by Cdks. J. Biol. Chem. 275: 29042–29052.

Masai, H., C. Taniyama, K. Ogino, E. Matsui, N. Kakusho et al., 2006 Phosphorylation of MCM4 by Cdc7 kinase facilitates its interaction with Cdc45 on the chromatin. J. Biol. Chem. 281: 39249–39261.

Matsumoto, S., K. Ogino, E. Noguchi, P. Russell, and H. Masai, 2005 Hsk1-Dfp1/Him1, the Cdc7-Dbf4 kinase in Schizosaccharomyces pombe, associates with Swi1, a component of the replication fork protection complex. J. Biol. Chem. 280: 42536–42542.

Matsumoto, S., M. Shimmoto, N. Kakusho, M. Yokoyama, Y. Kanoh et al., 2010 Hsk1 kinase and Cdc45 regulate replication stress-induced checkpoint responses in fission yeast. Cell Cycle 9: 4627–4637.

Mattarocci, S., M. Shyian, L. Lemmens, P. Damay, D. M. Altintas et al., 2014 Rif1 Controls DNA replication timing in yeast through the PP1 Phosphatase Glc7. Cell Reports 7: 62–69.

Mayer, M. L., S. P. Gygi, R. Aebersold, and P. Hieter, 2001 Identification of RFC(Ctf18p, Ctf8p, Dcc1p): an alternative RFC complex required for sister chromatid cohesion in S. cerevisiae. Mol. Cell 7: 959–970.

Memisoglu, A., and L. Samson, 2000   Contribution of base excision repair, nucleotide excision repair, and DNA recombination to alkylation resistance of the fission yeast Schizosaccharomyces pombe. J. Bacteriol. 182: 2104–2112.

Moyer, S. E., P. W. Lewis, and M. R. Botchan, 2006   Isolation of the Cdc45/Mcm2–7/GINS (CMG) complex, a candidate for the eukaryotic DNA replication fork helicase. Proc. Natl. Acad. Sci. USA 103: 10236–10241.

Muris, D. F., K. Vreeken, A. M. Carr, B. C. Broughton, A. R. Lehmann et al., 1993   Cloning the RAD51 homologue of Schizosaccharomyces pombe. Nucleic Acids Res. 21: 4586–4591.

Nabeshima, K., T. Nakagawa, A. F. Straight, A. Murray, Y. Chikashige et al., 1998   Dynamics of centromeres during metaphase-anaphase transition in fission yeast: Dis1 is implicated in force balance in metaphase bipolar spindle. Mol. Biol. Cell 9: 3211–3225.

Nasmyth, K., and P. Nurse, 1981   Cell division cycle mutants altered in DNA replication and mitosis in the fission yeast Schizosaccharomyces pombe. Mol. Gen. Genet. 182: 119–124.

Neelsen, K. J., and M. Lopes, 2015   Replication fork reversal in eukaryotes: from dead end to dynamic response. Nat. Rev. Mol. Cell Biol. 16: 207–220.

Nitani, N., C. Yadani, H. Yabuuchi, H. Masukata, and T. Nakagawa, 2008   Mcm4 C-terminal domain of MCM helicase prevents excessive formation of single-stranded DNA at stalled replication forks. Proc. Natl. Acad. Sci. USA 105: 12973–12978.

Noguchi, E., C. Noguchi, L.-L. Du, and P. Russell, 2003   Swi1 prevents replication fork collapse and controls checkpoint kinase Cds1. Mol. Cell. Biol. 23: 7861–7874.

Noguchi, E., C. Noguchi, W. H. McDonald, J. R. Yates, and P. Russell, 2004   Swi1 and Swi3 are components of a replication fork protection complex in fission yeast. Mol. Cell. Biol. 24: 8342–8355.

O'Donnell, M., and H. Li, 2016   The Eukaryotic Replisome Goes Under the Microscope. Curr. Biol. 26: R247–R256.

Panigrahi, A. K., N. Zhang, S. K. Otta, and D. Pati, 2012   A cohesin–RAD21 interactome. Biochem. J. 442: 661–670.

Pasion, S. G., and S. L. Forsburg, 1999   Nuclear localization of Schizosaccharomyces pombe Mcm2/Cdc19p requires MCM complex assembly. Mol. Biol. Cell 10: 4043–4057.

Peace, J. M., A. Ter-Zakarian, and O. M. Aparicio, 2014   Rif1 regulates initiation timing of late replication origins throughout the S. cerevisiae genome. PLoS One 9: e98501.

Petronczki, M., B. Chwalla, M. F. Siomos, S. Yokobayashi, W. Helmhart et al., 2004   Sister-chromatid cohesion mediated by the alternative RF-CCtf18/Dcc1/Ctf8, the helicase Chl1 and the polymerase-alpha-associated protein Ctf4 is essential for chromatid disjunction during meiosis II. J. Cell Sci. 117: 3547–3559.

Rapp, J. B., C. Noguchi, M. M. Das, L. K. Wong, A. B. Ansbach et al., 2010   Checkpoint-dependent and -independent roles of Swi3 in replication fork recovery and sister chromatid cohesion in fission yeast. PLoS One 5: e13379.

Sabatinos, S. A., and S. L. Forsburg, 2010   Molecular genetics of Schizosaccharomyces pombe. Methods Enzymol. 470: 759–795.

Sabatinos, S. A., and S. L. Forsburg, 2015   Measuring DNA content by flow cytometry in fission yeast. Methods Mol. Biol. 1300: 79–97.

Sabatinos, S. A., M. D. Green, and S. L. Forsburg, 2012   Continued DNA synthesis in replication checkpoint mutants leads to fork collapse. Mol. Cell. Biol. 32: 4986–4997.

Sabatinos, S. A., N. S. Ranatunga, J.-P. Yuan, M. D. Green, and S. L. Forsburg, 2015   Replication stress in early S phase generates apparent micronuclei and chromosome rearrangement in fission yeast. Mol. Biol. Cell 26: 3439–3450.

Sherman, D. A., S. G. Pasion, and S. L. Forsburg, 1998   Multiple domains of fission yeast Cdc19p (MCM2) are required for its association with the core MCM complex. Mol. Biol. Cell 9: 1833–1845.

Sheu, Y.-J., and B. Stillman, 2006   Cdc7-Dbf4 phosphorylates MCM proteins via a docking site-mediated mechanism to promote S phase progression. Mol. Cell 24: 101–113.

Sheu, Y.-J., and B. Stillman, 2010   The Dbf4-Cdc7 kinase promotes S phase by alleviating an inhibitory activity in Mcm4. Nature 463: 113–117.

Sheu, Y.-J., J. B. Kinney, A. Lengronne, P. Pasero, and B. Stillman, 2014   Domain within the helicase subunit Mcm4 integrates multiple kinase signals to control DNA replication initiation and fork progression. Proc. Natl. Acad. Sci. USA 111: E1899–E1908.

Shima, N., A. Alcaraz, I. Liachko, T. R. Buske, C. A. Andrews et al., 2007   A viable allele of Mcm4 causes chromosome instability and mammary adenocarcinomas in mice. Nat. Genet. 39: 93–98.

Simon, A. C., J. C. Zhou, R. L. Perera, F. van Deursen, C. Evrin et al., 2014   A Ctf4 trimer couples the CMG helicase to DNA polymerase α in the eukaryotic replisome. Nature 510: 293–297.

Snaith, H. A., G. W. Brown, and S. L. Forsburg, 2000   Schizosaccharomyces pombe Hsk1p is a potential cds1p target required for genome integrity. Mol. Cell. Biol. 20: 7922–7932.

Sommariva, E., T. K. Pellny, N. Karahan, S. Kumar, J. A. Huberman et al., 2005   Schizosaccharomyces pombe Swi1, Swi3, and Hsk1 are components of a novel S-phase response pathway to alkylation damage. Mol. Cell. Biol. 25: 2770–2784.

Stewart, E., C. R. Chapman, F. Al-Khodairy, and A. M. Carr, 1997   rqh1+, a fission yeast gene related to the Bloom's and Werner's syndrome genes, is required for reversible S phase arrest. Eur. Mol. Biol. Organ. J. 16: 2682–2692.

Sun, J., Y. Shi, R. E. Georgescu, Z. Yuan, B. T. Chait et al., 2015   The architecture of a eukaryotic replisome. Nat. Struct. Mol. Biol. 22: 1–9.

Thelander, L., and P. Reichard, 1979   Reduction of ribonucleotides. Annu. Rev. Biochem. 48: 133–158.

Tye, B. K., 1999   Minichromosome maintenance as a genetic assay for defects in DNA replication. Methods 18: 329–334.

Ulrich, H. D., and H. Walden, 2010   Ubiquitin signalling in DNA replication and repair. Nat. Rev. Mol. Cell Biol. 11: 479–489.

Walworth, N. C., and R. Bernards, 1996   rad-dependent response of the chk1-encoded protein kinase at the DNA damage checkpoint. Science 271: 353–356.

Wang, S. W., A. Goodwin, I. D. Hickson, and C. J. Norbury, 2001   Involvement of Schizosaccharomyces pombe Srs2 in cellular responses to DNA damage. Nucleic Acids Res. 29: 2963–2972.

Waseem, N. H., K. Labib, P. Nurse, and D. P. Lane, 1992   Isolation and analysis of the fission yeast gene encoding polymerase delta accessory protein PCNA. Eur. Mol. Biol. Organ. J. 11: 5111–5120.

Williams, D. R., and J. R. McIntosh, 2002   mcl1+, the Schizosaccharomyces pombe homologue of CTF4, is important for chromosome replication, cohesion, and segregation. Eukaryot. Cell 1: 758–773.

Willis, N., and N. Rhind, 2009   Regulation of DNA replication by the S-phase DNA damage checkpoint. Cell Div. 4: 13.

Wyatt, M. D., and D. L. Pittman, 2006   Methylating agents and DNA repair responses: Methylated bases and sources of strand breaks. Chem. Res. Toxicol. 19: 1580–1594.

Xu, D., P. Muniandy, E. Leo, J. Yin, S. Thangavel et al., 2010   Rif1 provides a new DNA-binding interface for the Bloom syndrome complex to maintain normal replication. EMBO J. 29: 3140–3155.

Xu, H., C. Boone, and G. W. Brown, 2007   Genetic dissection of parallel sister-chromatid cohesion pathways. Genetics 176: 1417–1429.

Yamazaki, S., M. Hayano, and H. Masai, 2013   Replication timing regulation of eukaryotic replicons: Rif1 as a global regulator of replication timing. Trends Genet. 29: 449–460.

Yun, J., S.-H. Song, J.-Y. Kang, J. Park, H.-P. Kim et al., 2016   Reduced cohesin destabilizes high-level gene amplification by disrupting pre-replication complex bindings in human cancers with chromosomal instability. Nucleic Acids Res. 44: 558–572.

Zaaijer, S., N. Shaikh, R. K. Nageshan, and J. P. Cooper, 2016   Rif1 Regulates the Fate of DNA Entanglements during Mitosis. Cell Reports 16: 148–160.

Communicating editor: C. S. Hoffman